carrying a limited number of genes from human chromosome 21. Transgenic Res 23:317–329

Moro M, Cecconi V, Martinoli C, Dallegno E, Giabbai B, Degano M, Glaichenhaus N, Protti MP, Dellabona P, Casorati G (2005) Generation of functional HLA-DR*1101 tetramers receptive for loading with pathogen or tumour derived synthetic peptides. BMC Immunol 6:24

Nakayama M, Ohara O (2005) Improvement of recombination efficiency by mutation of Red proteins. Biotechniques 38:917–924

Ohtsuka M, Ogiwara S, Miura H, Mizutani A, Warita T, Sato M, Imai K, Hozumi K, Sato T, Tanaka M, Kimura M, Inoko H (2010) Pronuclear injection-based mouse targeted transgenesis for reproducible and highly efficient transgene expression. Nucleic Acids Res 38:e198

Ohtsuka M, Miura H, Sato M, Kimura M, Inoko H, Gurumurthy CB (2012) PITT: pronuclear injection-based targeted transgenesis, a reliable transgene expression method in mice. Exp Anim 61:489–502

Ohzeki J, Bergmann JH, Kouprina N, Noskov VN, Nakano M, Kimura H, Earnshaw WC, Larionov V, Masumoto H (2012) Breaking the HAC barrier: histone H3K9 acetyl/methyl balance regulates CENP-A assembly. EMBO J 31:2391–2402

Pinkert CA, Widera G, Cowing C, Heber-Katz E, Palmiter RD, Flavell RA, Brinster RL (1985) Tissue-specific, inducible and functional expression of the E alpha d MHC class II gene in transgenic mice. EMBO J 4:2225–2230

Suzuki E, Nakayama M (2011) VCre/VloxP and SCre/SloxP: new site-specific recombination systems for genome engineering. Nucleic Acids Res 39:e49

Suzuki N, Nishii K, Okazaki T, Ikeno M (2006) Human artificial chromosomes constructed using the bottom-up strategy are stably maintained in mitosis and efficiently transmissible to progeny mice. J Biol Chem 281:26615–26623

Suzuki M, Takahashi T, Katano I, Ito R, Ito M, Harigae H, Ishii N, Sugamura K (2012) Induction of human humoral immune responses in a novel HLA-DR-expressing transgenic NOD/Shi-scid/γcnull mouse. Int Immunol 24:243–252

Vintersten K, Testa G, Naumann R, Anastassiadis K, Stewart AF (2008) Bacterial artificial chromosome transgenesis through pronuclear injection of fertilized mouse oocytes. Methods Mol Biol 415:83–100

Aicardi-Goutières Syndrome Is Caused by *IFIH1* Mutations

Hirotsugu Oda,[1,2] Kenji Nakagawa,[1] Junya Abe,[1,3] Tomonari Awaya,[1] Masahide Funabiki,[4] Atsushi Hijikata,[5] Ryuta Nishikomori,[1,*] Makoto Funatsuka,[6] Yusei Ohshima,[7] Yuji Sugawara,[8] Takahiro Yasumi,[1] Hiroki Kato,[4,9] Tsuyoshi Shirai,[5] Osamu Ohara,[2,10] Takashi Fujita,[4] and Toshio Heike[1]

Aicardi-Goutières syndrome (AGS) is a rare, genetically determined early-onset progressive encephalopathy. To date, mutations in six genes have been identified as etiologic for AGS. Our Japanese nationwide AGS survey identified six AGS-affected individuals without a molecular diagnosis; we performed whole-exome sequencing on three of these individuals. After removal of the common polymorphisms found in SNP databases, we were able to identify *IFIH1* heterozygous missense mutations in all three. In vitro functional analysis revealed that *IFIH1* mutations increased type I interferon production, and the transcription of interferon-stimulated genes were elevated. *IFIH1* encodes MDA5, and mutant MDA5 lacked ligand-specific responsiveness, similarly to the dominant *Ifih1* mutation responsible for the SLE mouse model that results in type I interferon overproduction. This study suggests that the *IFIH1* mutations are responsible for the AGS phenotype due to an excessive production of type I interferon.

Aicardi-Goutières syndrome (AGS [MIM 225750]) is a rare, genetically determined early-onset progressive encephalopathy.[1] Individuals affected with AGS typically suffer from progressive microcephaly associated with severe neurological symptoms, such as hypotonia, dystonia, seizures, spastic quadriplegia, and severe developmental delay.[2] On brain imaging, AGS is characterized by basal ganglia calcification, white matter abnormalities, and cerebral atrophy.[3,4] Cerebrospinal fluid (CSF) analyses show chronic lymphocytosis and elevated levels of IFN-α and neopterin.[3–5] AGS-affected individuals are often misdiagnosed as having intrauterine infections, such as TORCH syndrome, because of the similarities of these disorders, particularly the intracranial calcifications.[1] In AGS, etiological mutations have been reported in the following six genes: *TREX1* (MIM 606609), which encodes a DNA exonuclease; *RNASEH2A* (MIM 606034), *RNASEH2B* (MIM 610326), and *RNASEH2C* (MIM 610330), which together comprise the RNase H2 endonuclease complex; *SAMHD1* (MIM 606754), which encodes a deoxynucleotide triphosphohydrolase; and *ADAR1* (MIM 146920), which encodes an adenosine deaminase.[6–9] Although more than 90% of AGS-affected individuals harbor etiological mutations in one of these six genes, some AGS-affected individuals presenting with the clinical characteristics of AGS still lack a genetic diagnosis, suggesting the existence of additional AGS-associated genes.[1]

We recently conducted a nationwide survey of AGS in Japan and reported 14 AGS-affected individuals.[10] We have since recruited three other Japanese AGS-affected individuals, and among these 17 individuals, we have identified 11 individuals with etiologic mutations; namely, *TREX1* mutations in six, *SAMHD1* mutations in three, and *RNASEH2A* and *RNASEH2B* mutations in one each. Of the remaining six individuals without a molecular diagnosis, trio-based whole-exome sequencing was performed in three whose parents also agreed to participate in further genome-wide analyses (Figure 1A). Genomic DNA from each individual and the parents was enriched for protein-coding sequences, followed by massively parallel sequencing. The extracted nonsynonymous or splice-site variants were filtered to remove those with minor allele frequencies (MAF) > 0.01 in dbSNP137. To detect de novo variants, any variants observed in family members, listed in Human Genetic Variation Database (HGVD), or with MAF > 0.02 in our in-house exome database were removed. To detect autosomal-recessive (AR), compound heterozygous (CH), or X-linked (XL) variants, those with MAF > 0.05 in our in-house database were removed (Figure S1 available online). All samples were collected with the written informed consents by parents, and the study protocol was approved by the ethical committee of Kyoto University Hospital in accordance with the Declaration of Helsinki.

After common polymorphisms were removed, we identified a total of 40, 18, 89, and 22 candidate variants under the de novo, AR, CH, and XL inheritance models, respectively, that were present in at least one of the three individuals (Table S1). Among them, missense mutations were identified in *IFIH1* (MIM 606951, RefSeq accession

[1]Department of Pediatrics, Kyoto University Graduate School of Medicine, Kyoto 6068507, Japan; [2]Laboratory for Integrative Genomics, RIKEN Center for Integrative Medical Sciences, Yokohama 2300045, Japan; [3]Department of Pediatrics, Kitano Hospital, Tazuke Kofukai Medical Research Institute, Osaka 5308480, Japan; [4]Laboratory of Molecular Genetics, Institute for Virus Research, Kyoto University, Kyoto 6068507, Japan; [5]Department of Bioscience, Nagahama Institute of Bio-Science and Technology, Nagahama 5260829, Japan; [6]Department of Pediatrics, Tokyo Women's Medical University, Tokyo 1628666, Japan; [7]Department of Pediatrics, Faculty of Medical Sciences, University of Fukui, Fukui 9108507, Japan; [8]Department of Pediatrics and Developmental Biology, Graduate School of Medical and Dental Sciences, Tokyo Medical and Dental University, Tokyo 1138510, Japan; [9]Precursory Research for Embryonic Science and Technology (PRESTO), Science and Technology Agency (JST), Kawaguchi 3320012, Japan; [10]Department of Human Genome Research, Kazusa DNA Research Institute, Kisarazu 2920818, Japan
*Correspondence: mishiko@kuhp.kyoto-u.ac.jp
http://dx.doi.org/10.1016/j.ajhg.2014.06.007.

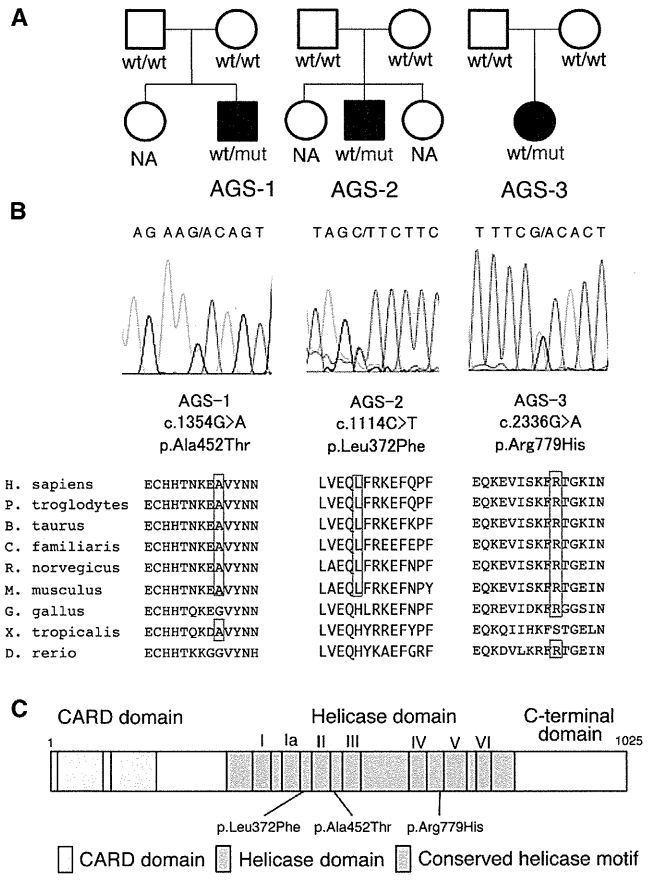

Figure 1. Pedigree Information for the AGS-Affected Individuals and Details of the *IFIH1* Mutations Identified

(A) The pedigrees of the three families indicating the AGS probands.

(B) Sanger sequencing chromatograms of the three *IFIH1* mutations found in the AGS-affected individuals. The locations of these mutations in the amino acid sequence of the MDA5 protein are shown in alignment with the conserved amino acid sequences from several species. This alignment was obtained via ClustalW2. The amino acids that are conserved with human are circled in red.

(C) The MDA5 protein domain structure with the amino acid substitutions observed in these AGS-affected individuals.

number NM_022168.2), which encodes MDA5 (RefSeq NP_071451.2). These missense mutations are c.1354G>A (p.Ala452Thr) in AGS-1; c.1114C>T (p.Leu372Phe) in AGS-2; and c.2336G>A (p.Arg779His) in AGS-3 (Figure 1B). None of the mutations are found in HGVD, including the 1,208 Japanese samples, or our in-house exome database of 312 Japanese individuals. Multiple-sequence alignment by ClustalW2 revealed that each of the amino acids affected by these mutations are conserved among mammals (Figure 1B). The subsequent amino acid alterations were all suggested to be disease causing in at least one of the four function-prediction programs used (Table 1). None of the other genes identified in the de novo inheritance model, or any of the genes identified in the other three inheritance models, were mutated in all three individuals. The *IFIH1* mutations identified were validated by Sanger sequencing. The other coding exons of *IFIH1* were also examined by Sanger sequencing, and no other mutations were found.

MDA5 is one of the cytosolic pattern recognition receptors that recognizes double-stranded RNA (dsRNA).[11] MDA5 consists of N-terminal tandem CARD domains, a central helicase domain, and a C-terminal domain (Figure 1C). When bound to dsRNA, MDA5 forms a closed, C-shaped ring structure around the dsRNA stem and excludes the tandem CARD as well as creates filamentous oligomer on dsRNA.[12] It is hypothesized that the tandem CARD interacts each other and activates MAVS on the mitochondrial outer membrane. Oligomerization of MAVS induces TBK1 activation, IRF3 phosphorylation, and induction of type I interferon transcription, resulting in the activation of a large number of interferon-stimulated genes (ISGs).

The neurological findings of the individuals with these *IFIH1* mutations are typical of AGS (Table S2). They were born with appropriate weights for their gestational ages without any signs of intrauterine infection. However, they all demonstrated severe developmental delay in early infancy associated with progressive microcephaly. No arthropathy, hearing loss, or ophthalmological problems were observed. As for extraneural features, all three individuals had at least one of the following autoimmune features: positivity for autoantibodies, hyperimmunoglobulinemia, hypocomplementemia, and thrombocytopenia. Notably, none of the individuals with *IFIH1* mutations had chilblain lesions, although all the five individuals with *TREX1* mutations and two of the three individuals with *SAMHD1* mutations in the Japanese AGS cohort showed chilblain lesions.[10] Individuals with *SAMHD1* mutations and *IFIH1* mutations both show autoimmune features; however, chilblain lesions have been observed only in individuals with *SAMHD1* mutations.[10]

To predict the effects of the identified amino acid substitutions on MDA5, three-dimensional model structures of MDA5 mutants were generated from the crystal structure of human MDA5-dsRNA complex[12] (Protein Data Bank [PDB] code 4gl2), using PyMOL (Schroedinger) and MOE (Chemical Computing Group) (Figure S2A). The oligomeric model of MDA5 was generated using the electron microscopy imaging data of MDA5 filament lacking CARD domain[13] (Electron Microscopic Data Bank [EMDB] code 5444) (Figure S2B). The three amino acid substitutions in the AGS-affected individuals are all located within the helicase domain (Figures 1C and S2A). Because Ala452 directly contacts the dsRNA ribose O2′ atom, the p.Ala452Thr substitution probably affects the binding affinity to dsRNA due to an atomic repulsion between the side chain of Thr452 and the dsRNA O2′ atom (Figures S2C and S2D). Leu372 is located adjacent to the ATP binding pocket, and the p.Leu372Phe substitution could increase the side chain volume of the binding pocket, affecting its ATP hydrolysis activity (Figures S2E and S2F). In our oligomeric model, Arg779 is located at the interface between the two monomers, which is consistent with the

Table 1. Functional Predictions of the *IFIH1* Variants

Individuals	Nucleotide Change	Amino Acid Change	SIFT	PolyPhen2	Mutation Taster	PROVEAN
AGS-1	c.1354G>A	p.Ala452Thr	tolerated	benign	disease causing	neutral
AGS-2	c.1114C>T	p.Leu372Phe	tolerated	probably damaging	disease causing	neutral
AGS-3	c.2336G>A	p.Arg779His	tolerated	probably damaging	disease causing	deleterious

The potential functional effects of the *IFIH1* variants identified in the AGS-affected individuals were predicted via SIFT, PolyPhen2, Mutation Taster, and PROVEAN.

recent report showing that Lys777, close to Arg779, is in close proximity to the adjacent monomer.[12] Furthermore, in our model, Arg779 is in close to Asp572 on the surface of the adjacent monomer. We speculate that losing the positive charge due to the p.Arg779His substitution would possibly affect the electrostatic interaction between the MDA5 monomers (Figures S2G and S2H).

To connect the identified *IFIH1* mutations with the AGS phenotype, we examined the type I interferon signature in the individuals by performing quantitative RT-PCR (qRT-PCR) of seven ISGs.[14] Peripheral blood mononuclear cells (PBMCs) from the three AGS-affected individuals showed upregulation of ISG transcription (Figure 2), confirming the type I interferon signature in the individuals with *IFIH1* mutations.

To elucidate the disease-causing capability of the identified *IFIH1* mutations, three FLAG-tagged *IFIH1* mutant plasmids containing these mutations were constructed via site-directed mutagenesis. These plasmids were transiently expressed on human hepatoma cell line Huh7 and the *IFNB1* promoter activity as well as endogenous expression of *IFIT1* (MIM 147690) was measured 48 hr after transfection.[15] The three mutant plasmids activated the *IFNB1* promoter in Huh7 cells more strongly than the wild MDA5 and nearby missense variants reported in dbSNP (Figures 3 and S3). The upregulation of endogenous *IFIT1* was also observed in the transfected cells (Figure S4), suggesting that these AGS mutations enhance the intrinsic activation function of MDA5. Recent genome-wide association studies (GWASs) showed association of the *IFIH1* with various autoimmune diseases, such as systemic lupus erythematosus (SLE), type I diabetes, psoriasis, and vitiligo.[16–19] We examined *IFNB1* promoter activity induced by the c.2836G>A (p.Ala946Thr) polymorphism (rs1990760) identified in the GWASs. Although the c.2836G>A polymorphism partially activated the promoter activity, the induced activity was lower than those of the AGS-derived mutants. In addition, the dominantly inherited SLE mouse model in the ENU-treated mouse colony is reported to have the *Ifih1* mutation, c.2461G>A (p.Gly821Ser).[15] These observations suggest that *IFIH1* has strong association with various autoimmune diseases, especially SLE, which also has a type I interferon signature.[20] Because alteration of *TREX1* has been reported to cause AGS as well as SLE,[21] it seems quite plausible for *IFIH1* to also be involved in both AGS and SLE. Interestingly, all the individuals identified with *IFIH1* mutations had autoantibodies, suggesting the contribution of *IFIH1* mutations to autoimmune phenotypes.

To further delineate the functional consequences of the three *IFH1* mutations, we measured the ligand-specific *Ifnb* mRNA induction by stimulating *Ifih1*^{null} mouse embryonic fibroblasts (MEFs) reconstituted with retrovirus expressing the *IFIH1* mutants by an MDA5-specific ligand, encephalomyocarditis virus (EMCV).[22] None of the MEF cells expressing the three mutant *IFIH1* responded to the EMCV, which suggested that the MDA5 variants lacked the ligand-specific responsiveness. The response of the three AGS mutants against the MDA5-specific EMCV was similar to that of the p.Gly821Ser variant reported in the dominantly inherited SLE mouse model with type I interferon overproduction[15] (Figures 4 and S5).

During the revision of this manuscript, Rice et al. identified nine individuals with *IFIH1* mutations, including the c.2336G>A mutation we identified, in a spectrum of neuroimmunological features consistently associated with enhanced type I interferon states including AGS.[23] Although we agree that the *IFIH1* mutations cause constitutive type I interferon activation, Rice et al. show that the mutated MDA5 proteins maintain ligand-induced responsiveness, which was not the case in our study. Because we measured the ligand-specific responsiveness of MDA5 in different experimental conditions, further analysis remains to be performed to reveal the biochemical mechanism of interferon overproduction by the mutated MDA5.

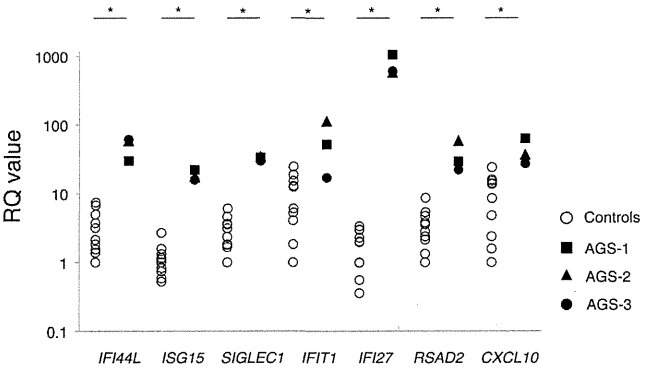

Figure 2. Quantitative RT-PCR of a Panel of Seven ISGs in PBMCs Obtained from the *IFIH1*-Mutated Individuals and Healthy Control Subject

qRT-PCR was performed as previously described.[15] The relative abundance of each transcript was normalized to the expression level of β-actin. Taqman probes used were the same as previous report,[14] except for *ACTB* (MIM 102630). Individual data were shown relative to a single calibrator (control 1). The experiment was performed in triplicate. Statistical significance was determined by Mann-Whitney U test, *$p < 0.05$.

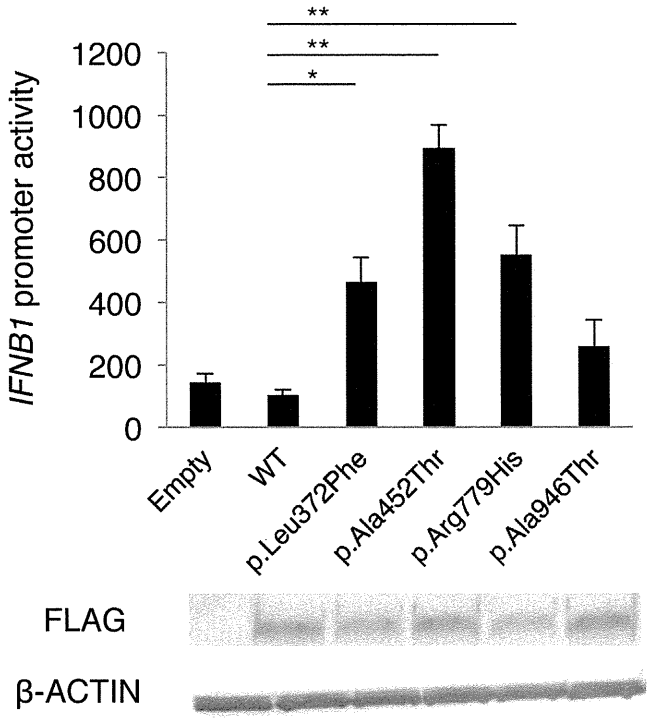

Figure 3. The Effects of the Three MDA5 Variants on *IFNB1* Expression

Huh7 cells were transfected with a reporter gene containing *IFNB1* promoter (p-55C1B Luc), an empty vector (BOS), and expression vectors for FLAG-tagged human wild-type *IFIH1*, c.2836G>A polymorphism (p.Ala946Thr) in the GWASs, and the identified *IFIH1* mutants. Luciferase activity was measured 48 hr after transfection, and the MDA5 protein accumulation was examined by immunoblotting as previously described.[15] FLAG indicates the accumulation of FLAG-tagged MDA5. Each experiment was performed in triplicate and data are mean ± SEM. Shown is a representative of two with consistent results. Statistical significance was determined by Student's t test. *$p < 0.05$, **$p < 0.01$.

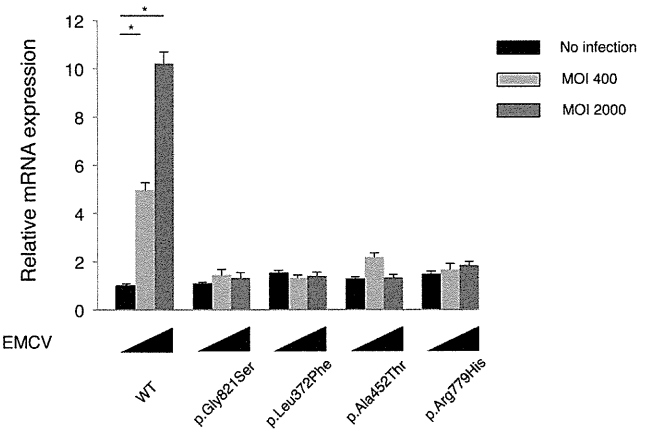

Figure 4. *Ifnb* mRNA Levels in *Ifih1*-Deficient MEFs Expressing *IFIH1* Mutants

The MEFs were infected with retroviruses encoding mouse wild-type *Ifih1*, mouse *Ifih1* with c.2461G>A (p.Gly821Ser) (RefSeq NM_027835.3) mutation, or the three AGS mutants of human *IFIH1*. At 48 hr after the retroviral infection, these MEFs were infected with indicated multiplicity of infection (MOI) of EMCV for 6 hr, and *Ifnb* mRNA levels were measured by qRT-PCR. The relative abundance of each transcript was normalized to the expression level of 18S ribosomal RNA. Data are shown as mean ± SEM of triplicate samples. Shown is a representative of two independent experiments. Statistical significance was determined by Student's t test, *$p < 0.001$. The expression of the retrovirally transduced FLAG-tagged constructs was confirmed by immunoblotting (Figure S5).

In conclusion, we identified mutations in *IFIH1* as a cause of AGS. The individuals with the *IFIH1* mutations showed encephalopathy typical of AGS as well as the type I interferon signature with autoimmune phenotypes, but lacked the chilblains. Further analysis remains to elucidate the mechanism of how the *IFIH1* mutations identified in AGS cause the type I interferon overproduction.

Supplemental Data

Supplemental Data include five figures and two tables and can be found with this article online at http://dx.doi.org/10.1016/j.ajhg.2014.06.007.

Acknowledgments

We are very grateful to Y. Takaoka (Kyoto University) and E. Abe (RIKEN Center for Integrative Medical Sciences) for their technical assistance on Sanger sequencing, to E. Hirano (Kyoto University) for her technical assistance on functional analyses of the AGS mutants, to M. Takazawa (Kazusa DNA Research Institute) for his contribution to exome data analysis, and to T. Taylor for his critical reading of the manuscript. This work was supported by the Platform for Drug Discovery, Informatics, and Structural Life Science from the Ministry of Education, Culture, Sports, Science and Technology, Japan. This work was supported by Grants-in-aid for Scientific Research from the Japanese Ministry of Health, Labor and Welfare and the Japanese Ministry of Education, Culture, Sports, Science, Technology (MEXT).

Received: March 1, 2014
Accepted: June 11, 2014
Published: July 3, 2014

Web Resources

The URLs for the data presented herein are as follows:

Burrows-Wheeler Aligner, http://bio-bwa.sourceforge.net/
ClustalW2, http://www.ebi.ac.uk/Tools/msa/clustalw2/
dbSNP, http://www.ncbi.nlm.nih.gov/projects/SNP/
EMDataBank, http://www.emdatabank.org/index.html
GATK, http://www.broadinstitute.org/gatk/
Human Genetic Variation Database (HGVD), http://www.genome.med.kyoto-u.ac.jp/SnpDB/
MutationTaster, http://www.mutationtaster.org/
Online Mendelian Inheritance in Man (OMIM), http://www.omim.org/
PolyPhen-2, http://www.genetics.bwh.harvard.edu/pph2/
PROVEAN, http://provean.jcvi.org/index.php
RCSB Protein Data Bank, http://www.rcsb.org/pdb/home/home.do
RefSeq, http://www.ncbi.nlm.nih.gov/RefSeq
SIFT, http://sift.bii.a-star.edu.sg/

References

1. Chahwan, C., and Chahwan, R. (2012). Aicardi-Goutieres syndrome: from patients to genes and beyond. Clin. Genet. *81*, 413–420.
2. Ramantani, G., Kohlhase, J., Hertzberg, C., Innes, A.M., Engel, K., Hunger, S., Borozdin, W., Mah, J.K., Ungerath, K., Walkenhorst, H., et al. (2010). Expanding the phenotypic spectrum of lupus erythematosus in Aicardi-Goutières syndrome. Arthritis Rheum. *62*, 1469–1477.
3. Orcesi, S., La Piana, R., and Fazzi, E. (2009). Aicardi-Goutieres syndrome. Br. Med. Bull. *89*, 183–201.
4. Rice, G., Patrick, T., Parmar, R., Taylor, C.F., Aeby, A., Aicardi, J., Artuch, R., Montalto, S.A., Bacino, C.A., Barroso, B., et al. (2007). Clinical and molecular phenotype of Aicardi-Goutieres syndrome. Am. J. Hum. Genet. *81*, 713–725.
5. Blau, N., Bonafé, L., Krägeloh-Mann, I., Thöny, B., Kierat, L., Häusler, M., and Ramaekers, V. (2003). Cerebrospinal fluid pterins and folates in Aicardi-Goutières syndrome: a new phenotype. Neurology *61*, 642–647.
6. Crow, Y.J., Hayward, B.E., Parmar, R., Robins, P., Leitch, A., Ali, M., Black, D.N., van Bokhoven, H., Brunner, H.G., Hamel, B.C., et al. (2006). Mutations in the gene encoding the 3′-5′ DNA exonuclease TREX1 cause Aicardi-Goutières syndrome at the AGS1 locus. Nat. Genet. *38*, 917–920.
7. Crow, Y.J., Leitch, A., Hayward, B.E., Garner, A., Parmar, R., Griffith, E., Ali, M., Semple, C., Aicardi, J., Babul-Hirji, R., et al. (2006). Mutations in genes encoding ribonuclease H2 subunits cause Aicardi-Goutières syndrome and mimic congenital viral brain infection. Nat. Genet. *38*, 910–916.
8. Rice, G.I., Bond, J., Asipu, A., Brunette, R.L., Manfield, I.W., Carr, I.M., Fuller, J.C., Jackson, R.M., Lamb, T., Briggs, T.A., et al. (2009). Mutations involved in Aicardi-Goutières syndrome implicate SAMHD1 as regulator of the innate immune response. Nat. Genet. *41*, 829–832.
9. Rice, G.I., Kasher, P.R., Forte, G.M., Mannion, N.M., Greenwood, S.M., Szynkiewicz, M., Dickerson, J.E., Bhaskar, S.S., Zampini, M., Briggs, T.A., et al. (2012). Mutations in ADAR1 cause Aicardi-Goutières syndrome associated with a type I interferon signature. Nat. Genet. *44*, 1243–1248.
10. Abe, J., Nakamura, K., Nishikomori, R., Kato, M., Mitsuiki, N., Izawa, K., Awaya, T., Kawai, T., Yasumi, T., Toyoshima, I., et al. (2014). A nationwide survey of Aicardi-Goutieres syndrome patients identifies a strong association between dominant TREX1 mutations and chilblain lesions: Japanese cohort study. Rheumatology *53*, 448–458.
11. Yoneyama, M., and Fujita, T. (2009). RNA recognition and signal transduction by RIG-I-like receptors. Immunol. Rev. *227*, 54–65.
12. Wu, B., Peisley, A., Richards, C., Yao, H., Zeng, X., Lin, C., Chu, F., Walz, T., and Hur, S. (2013). Structural basis for dsRNA recognition, filament formation, and antiviral signal activation by MDA5. Cell *152*, 276–289.
13. Berke, I.C., Yu, X., Modis, Y., and Egelman, E.H. (2012). MDA5 assembles into a polar helical filament on dsRNA. Proc. Natl. Acad. Sci. USA *109*, 18437–18441.
14. Rice, G.I., Forte, G.M., Szynkiewicz, M., Chase, D.S., Aeby, A., Abdel-Hamid, M.S., Ackroyd, S., Allcock, R., Bailey, K.M., Balottin, U., et al. (2013). Assessment of interferon-related biomarkers in Aicardi-Goutières syndrome associated with mutations in TREX1, RNASEH2A, RNASEH2B, RNASEH2C, SAMHD1, and ADAR: a case-control study. Lancet Neurol. *12*, 1159–1169.
15. Funabiki, M., Kato, H., Miyachi, Y., Toki, H., Motegi, H., Inoue, M., Minowa, O., Yoshida, A., Deguchi, K., Sato, H., et al. (2014). Autoimmune disorders associated with gain of function of the intracellular sensor MDA5. Immunity *40*, 199–212.
16. Smyth, D.J., Cooper, J.D., Bailey, R., Field, S., Burren, O., Smink, L.J., Guja, C., Ionescu-Tirgoviste, C., Widmer, B., Dunger, D.B., et al. (2006). A genome-wide association study of nonsynonymous SNPs identifies a type 1 diabetes locus in the interferon-induced helicase (IFIH1) region. Nat. Genet. *38*, 617–619.
17. Gateva, V., Sandling, J.K., Hom, G., Taylor, K.E., Chung, S.A., Sun, X., Ortmann, W., Kosoy, R., Ferreira, R.C., Nordmark, G., et al. (2009). A large-scale replication study identifies TNIP1, PRDM1, JAZF1, UHRF1BP1 and IL10 as risk loci for systemic lupus erythematosus. Nat. Genet. *41*, 1228–1233.
18. Strange, A., Capon, F., Spencer, C.C., Knight, J., Weale, M.E., Allen, M.H., Barton, A., Band, G., Bellenguez, C., Bergboer, J.G., et al.; Genetic Analysis of Psoriasis Consortium & the Wellcome Trust Case Control Consortium 2 (2010). A genome-wide association study identifies new psoriasis susceptibility loci and an interaction between HLA-C and ERAP1. Nat. Genet. *42*, 985–990.
19. Jin, Y., Birlea, S.A., Fain, P.R., Ferrara, T.M., Ben, S., Riccardi, S.L., Cole, J.B., Gowan, K., Holland, P.J., Bennett, D.C., et al. (2012). Genome-wide association analyses identify 13 new susceptibility loci for generalized vitiligo. Nat. Genet. *44*, 676–680.
20. Bennett, L., Palucka, A.K., Arce, E., Cantrell, V., Borvak, J., Banchereau, J., and Pascual, V. (2003). Interferon and granulopoiesis signatures in systemic lupus erythematosus blood. J. Exp. Med. *197*, 711–723.
21. Lee-Kirsch, M.A., Gong, M., Chowdhury, D., Senenko, L., Engel, K., Lee, Y.A., de Silva, U., Bailey, S.L., Witte, T., Vyse, T.J., et al. (2007). Mutations in the gene encoding the 3′-5′ DNA exonuclease TREX1 are associated with systemic lupus erythematosus. Nat. Genet. *39*, 1065–1067.
22. Kato, H., Takeuchi, O., Sato, S., Yoneyama, M., Yamamoto, M., Matsui, K., Uematsu, S., Jung, A., Kawai, T., Ishii, K.J., et al. (2006). Differential roles of MDA5 and RIG-I helicases in the recognition of RNA viruses. Nature *441*, 101–105.
23. Rice, G.I., del Toro Duany, Y., Jenkinson, E.M., Forte, G.M., Anderson, B.H., Ariaudo, G., Bader-Meunier, B., Baildam, E.M., Battini, R., Beresford, M.W., et al. (2014). Gain-of-function mutations in IFIH1 cause a spectrum of human disease phenotypes associated with upregulated type I interferon signaling. Nat. Genet. *46*, 503–509.

Basophil-Derived Interleukin-4 Controls the Function of Natural Helper Cells, a Member of ILC2s, in Lung Inflammation

Yasutaka Motomura,[1,2] Hideaki Morita,[6] Kazuyo Moro,[3,5,7] Susumu Nakae,[8] David Artis,[9] Takaho A. Endo,[4] Yoko Kuroki,[4] Osamu Ohara,[4] Shigeo Koyasu,[3] and Masato Kubo[1,2,*]

[1]Division of Molecular Pathology, Research Institute for Biomedical Science, Tokyo University of Science, 2669 Yamazaki, Noda-shi, Chiba, 278-0022, Japan

[2]Laboratory for Cytokine Regulation

[3]Laboratory for Immune Cell System

[4]Laboratory for Integrative Genomics

RIKEN Center for Integrative Medical Sciences (IMS), 1-7-22 Suehiro-cho, Tsurumi-ku, Yokohama, Kanagawa 230-0045, Japan

[5]Division of Immunobiology, Department of Medical Life Science, Graduate School of Medical Life Science, Yokohama City University, 1-7-29 Suehiro-cho, Yokohama 230-0045, Japan

[6]Department of Allergy and Immunology, National Research Institute for Child Health and Development, Tokyo 157-8535, Japan

[7]Precursory Research for Embryonic Science and Technology (PRESTO), Japan Science and Technology Agency, 7 Goban-cho, Chiyoda-ku, Tokyo 102-0076, Japan

[8]Laboratory of Systems Biology, Center for Experimental Medicine and Systems Biology, The Institute of Medical Science, The University of Tokyo, 4-6-1 Shirokanedai, Minato-ku, Tokyo, 108-8639, Japan

[9]Department of Microbiology, Institute for Immunology, Perelman School of Medicine, University of Pennsylvania, 356 BRB, Philadelphia, PA 19104, USA

*Correspondence: raysolfc@rcai.riken.jp

http://dx.doi.org/10.1016/j.immuni.2014.04.013

SUMMARY

Allergic asthma is an inflammatory disease characterized by lung eosinophilia controlled by type 2 cytokines. Cysteine proteases are potent triggers of allergic inflammation by causing barrier disruption in lung epithelial cells inducing the elevation of interleukin-5 (IL-5) and IL-13 from natural helper (NH) cells, a member of ILC2s, which leads to lung eosinophilia. In this study, we found that basophils play a crucial role in NH cell-mediated eosinophilic inflammation induced by protease allergens. Conditional deletion of basophils caused a resolution of the papain-induced eosinophilia and mucus production. Resolution of eosinophilia was also observed in mice lacking IL-4 specifically in basophils, indicating that basophil-derived IL-4 enhanced expression of the chemokine CCL11, as well as IL-5, IL-9, and IL-13 in NH cells, thus attracting eosinophils. These results demonstrate that IL-4 from basophils has an important role in the NH-derived cytokine and chemokine expression, subsequently leading to protease allergen-induced airway inflammation.

INTRODUCTION

Allergen-induced asthma is a chronic inflammatory disease characterized by airway obstruction and wheezing and is thought to be positively controlled by type 2 cytokines, including interleukin-4 (IL-4), IL-5, and IL-13. IL-4 promotes immunoglobulin E (IgE) production by B cells (Coffman et al., 1986), IL-5 induces development, recruitment, and activation of eosinophils (Hamelmann and Gelfand, 2001), and IL-13 controls the effector phase of asthma by inducing airway remodeling and hyperresponsiveness of airway reaction, as well as hyperproduction of mucus (Wills-Karp, 2004). Conventional asthma mouse models have clearly indicated the importance of T helper 2 (Th2) cells, mast cells and eosinophilic inflammation (Kim et al., 2010). Asthmatic inflammation is also induced by allergen proteases, including those from papain and house dust mites (HDM). The HDM-derived protease Derp1 causes airway influx of eosinophils and bronchoconstriction in asthma patients (Gregory and Lloyd, 2011). A plant-derived cysteine protease, papain, causes occupational asthma (Novey et al., 1979). More recently, papain has been reported to induce adaptive Th2 cell-mediated immunity, which is initiated by basophil-derived IL-4 and cooperation between dermal dendritic cells (DCs) and basophils (Sokol et al., 2008; Tang et al., 2010). Meanwhile, papain can cause asthma-like airway inflammation in Rag-deficient mice (Oboki et al., 2010), suggesting the presence of Th2 cell-independent mechanisms. Proteases such as papain cause barrier disruption in epithelial cells, leading to the elevation of multiple cytokines including IL-25, IL-33, and thymic stromal lymphopoietin (TSLP) due to the stress of tissue injury. Moreover, intranasal (i.n.) administration of papain fails to induce eosinophil infiltration and mucus hyperproduction in the lungs of *Il33*$^{-/-}$ mice (Oboki et al., 2010). These results clearly demonstrate an importance of IL-33 in protease allergen-induced allergic inflammation.

Innate lymphocytes contributing to type 2 cytokine responses in vivo have been discovered in the gut-associated mucosal tissues (Moro et al., 2010; Neill et al., 2010; Price et al., 2010; Saenz

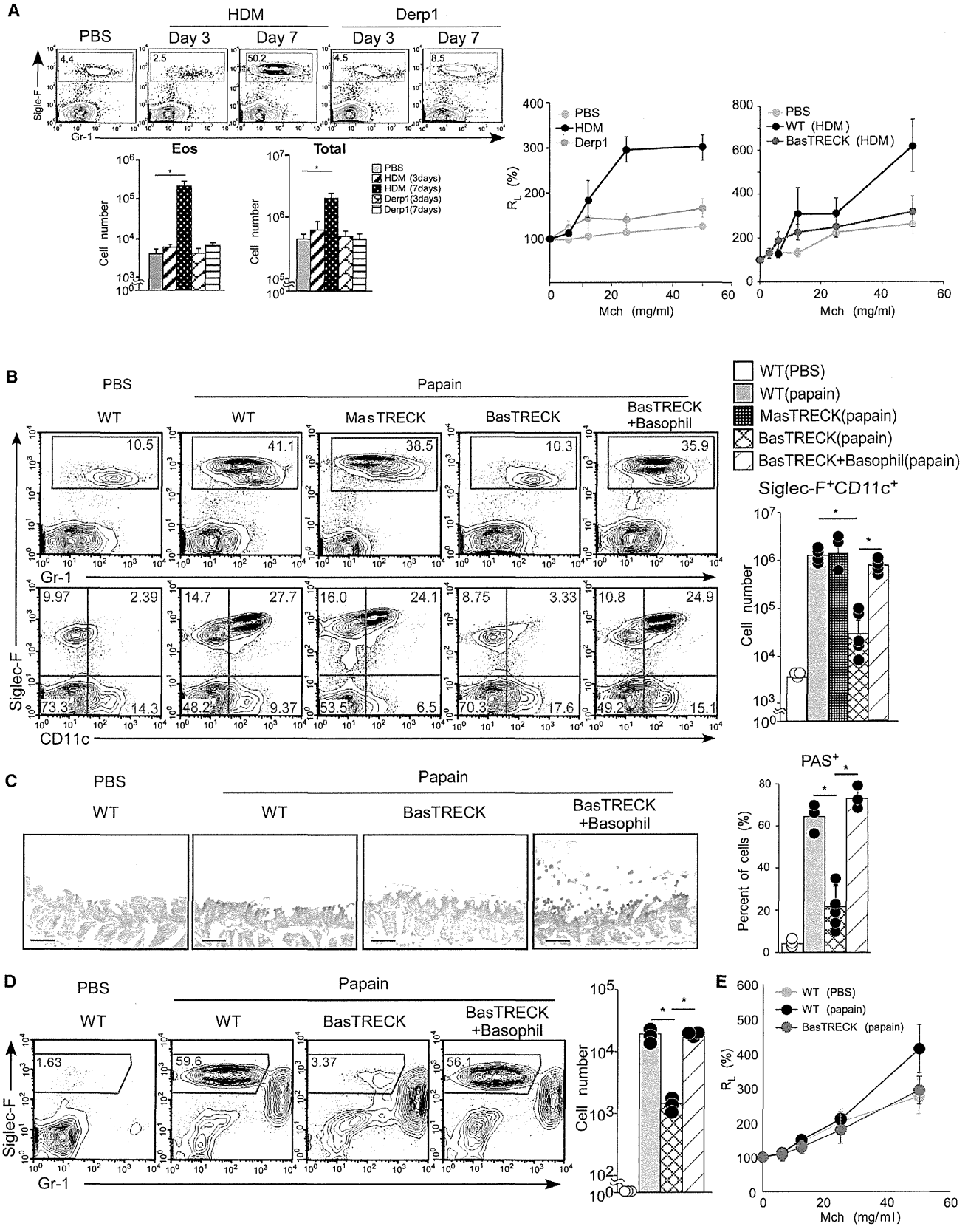

(legend on next page)

et al., 2010). These cells, which have been termed natural helper (NH) cells, nuocytes, and innate helper type 2 (Ih2) cells, are now classified as members of group 2 innate lymphoid cells (ILC2s) (Spits et al., 2013), or multipotent progenitor type 2 (MPP^{type2}) cells, and produce type 2 cytokines in response to epithelial cell-derived IL-25, IL-33, and TSLP. These innate lymphocytes have also been found in several other tissues including the liver, spleen, and lung (Price et al., 2010). The importance of NH cells has been reported in viral-induced airway inflammation in the lungs of virus-infected BALB/c mice (Chang et al., 2011). Furthermore, it has been suggested that IL-13-producing innate lymphocytes might play a role in lung eosinophilic inflammation and asthma (Kaiko and Foster, 2011; Kim et al., 2010; Lloyd and Hessel, 2010), and NH cells have been identified as a cell subset responsible for papain-induced lung inflammation (Halim et al., 2012). Papain induces acute eosinophilia in *Rag1*$^{-/-}$ mice, but not in *Rag2*$^{-/-}$*Il2rg*$^{-/-}$ mice that lack NH cells, indicating a critical contribution of lung NH cells to this process (Halim et al., 2012). Treatment of lungs with papain induces IL-33 and TSLP production by stromal cells, resulting in IL-5 and IL-13 production by lung NH cells. Thus, the IL-33-NH cell-IL-5 and IL-13 axis is thought to be a critical pathway for protease-induced airway inflammation.

Recently, the importance of basophils in chronic allergic responses and protective immunity against helminths has been reported (Pulendran and Artis, 2012), however, the role of basophils in Th2 cell-mediated induction has been controversial. It has been reported that basophils are essential for IgE-meditated chronic allergic dermatitis and for protection against infection with *N. brasiliensis* (Ohnmacht et al., 2010). Deletion of basophils in vivo with the MAR-1 antibody demonstrates that papain preferentially induces IL-4 expression by basophils and their transient recruitment into draining lymph nodes and that the basophil-derived IL-4 promotes Th2 cell differentiation (Sokol et al., 2008). Meanwhile, selective genetic depletion of basophils with the *Mcpt8cre* transgenic mouse model shows that basophils are dispensable for the induction of Th2 cell differentiation in the papain system (Ohnmacht et al., 2010). Moreover, the *Il4* reporter system with the *Il4* reporter mouse (*Il4*$^{tm1(CD2)Mmrs}$) also demonstrates basophil-independent Th2 cell priming in vivo (Sullivan et al., 2011).

We have established a diphtheria toxin (DT)-based conditional basophil deletion system, named BasTRECK (Sawaguchi et al., 2012). With this model, we have shown an indispensable role of basophils in IgE-mediated chronic allergic inflammation (IgE-CAI), allergic dermal response and eosinophilic esophagitis (EoE) but not in the induction of Th2 cell differentiation. Although IL-33 acts on murine basophils to induce high expression of IL-4 in vivo and in vitro (Kroeger et al., 2009; Schneider et al., 2009), the in vivo relevance of basophil-derived IL-4 remains unclear.

We have generated a series of mouse lines lacking *Il13* or *Il4* enhancer elements, *Il13* CGRE, *Il4* HS2, *Il4* 3′UTR, *Il4* HS4-deficient mice (Tanaka et al., 2011), and we found that the *Il4* 3′UTR-deficient mice were impaired in IL-4 expression specifically in basophils without affecting the IL-4 expression in Th2 and Tfh cells (Harada et al., 2012; Tanaka et al., 2011). Here we show that *Il4* 3′UTR-deficient mice were unable to induce NH cell activation, type 2 cytokine production, or lung eosinophilic inflammation upon papain treatment. These results indicate that IL-4 from basophils has an important role in the IL-33-NH cell-IL-5 and IL-13 axis leading to eosinophil-mediated airway inflammation.

RESULTS

Role of Basophils in Cysteine Protease-Induced Eosinophilic Inflammation

Derp1 and Derp2 are house dust mite (HDM) components of *Dermatophagoides pteronissinus* with cysteine protease activity that trigger airway inflammation (Tovey et al., 1981). Indeed, eosinophil infiltration and mucus formation and airway hyperresponsiveness (AHR) were induced by i.n. administration of HDM and to a lesser extent by recombinant Derp1 administration (Figure 1A). Papain, a plant-derived cysteine protease, has been reported to cause asthma-like airway inflammation (Novey et al., 1979), and indeed, i.n. administration of papain markedly induced the influx of Siglec-F^+CD11c^+ eosinophils into the broncho alveolar lavage (BAL) fluid, mucin formation, and airway hyperresponsiveness (Figures 1B–1E). Papain inhalation increased the number of activated $CD11c^+$ eosinophils, which was reflected in the upregulation of several inflammatory cytokines and chemokine genes (*Il6*, *Il13*, *Ccl7*, *Ccl11*), as well as complement components (*C1qb*, *C3*) and an antimicrobial peptide (*S100a4*) (see Figure S1 available online). These results indicate that papain promotes the conversion of eosinophil into $CD11c^+$ activated eosinophils.

Recent studies have revealed that innate cells play a substantial role in airway inflammation (Halim et al., 2012). Lung epithelial cells can produce multiple cytokines including IL-33 and thymic stromal lymphopoietin (TSLP), which induce IL-5 and IL-13 production and eosinophilic lung inflammation. IL-33 is constitutively expressed in the lung and further increased after papain treatment (Oboki et al., 2010). Papain-induced eosinophilic

Figure 1. Role of Basophils in Cysteine Protease-Induced Eosinophilic Lung Inflammation

(A) Flow cytometric analysis of eosinophils in the lung of WT i.n. administrated HDM or recombinant Derp1 continuously for 3 or 7 days (left upper). Quantification of eosinophils and total cells in the lung at 3 and 7 days (left lower). Airway hypersensitivity (AHR) to methacholine (Mch) in WT mice after HDM or Derp1 treatment (middle) and in DT-treated WT or BasTRECK mice after HDM treatment (right).

(B) Flow cytometric analysis of eosinophils in the lungs of DT-treated WT, MasTRECK, and BasTRECK mice i.n. administrated papain for 3 continuous days from day 7 (for MasTRECK mice) and day 1 (for BasTRECK mice after DT treatment. For reconstitution of basophils, before papain treatment the DT-treated BasTRECK mice were injected with basophils derived from papain-treated WT mice (left). The quantification of $CD11c^+$ eosinophils in the lung (right).

(C) Periodic acid Schiff (PAS) staining of lung tissues from the mice analyzed in (B). Scale bars represent 50 μm. The proportion of PAS-positive cells in the lung sections of the indicated mice (right). The bars in the graph are labeled as in (B).

(D) Flow cytometry of eosinophils in BAL fluid of the mice depicted in (B) (left). Quantification of $CD11c^+$ eosinophils in the lungs of the indicated mice (right). Bars in the graph of (B) and (C) are labeled as in (B).

(E) Airway hypersensitivity to Mch in DT-treated WT or BasTRECK mice after papain treatment. Dot plots are shown on cells gated out Propidium iodide $(PI)^+$Autofluorescence$^+Gr1^{hi}$ (A), (B), or PI^+Autofluorescence$^+$ (D). Results are representative of three independent experiments, and error bars represent the SEM.

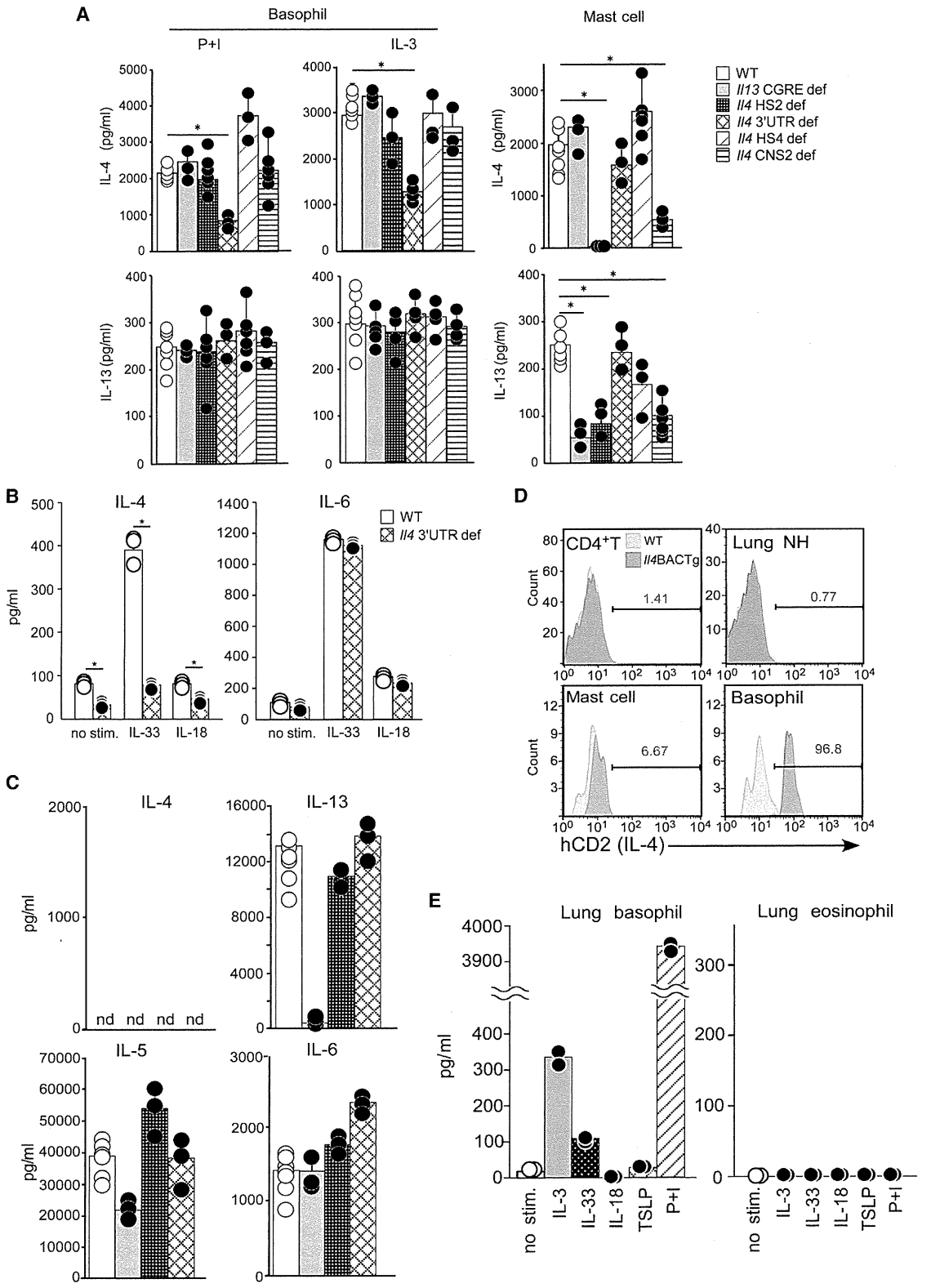

Figure 2. Deletion of the 3′UTR Region Selectively Impairs IL-4 Production by Basophils

(A) Bio-Plex analysis of IL-4 and IL-13 production by purified bone marrow basophils and peritoneal mast cells of the indicated mice in response to PMA plus Ionomycin (P+I) or rIL-3 stimulation for 24 hr.

(B) Bio-Plex analysis of IL-4 production by purified bone marrow basophils derived from WT and *Il4* 3′UTR-deficient mice in response to IL-18 and IL-33 for 24 hr.

(legend continued on next page)

lung inflammation was largely dependent on IL-33, but not TSLP (Figures S2A and S2B). A similar acute type of lung eosinophilia occurred in *Rag1*-deficient mice, which lacks all T and B cells, indicating that papain-induced lung inflammation can occur without T cell-derived cytokines. However, we observed small number of IL-13 expressing T cells that correspond to resident memory T cells, $CD4^+CD44^{hi}CD62L^{lo}CD69^+\alpha$Galcer-CD1d-dimer$^-$CXCR3$^-$CCR2$^-$ (Figures S2C, S3A, and S3B). Meanwhile, a large number of IL-13 expressing NH cells was observed in the lung (Figure S3A). These results suggest that IL-33 directly acts on NH cells, mast cells, and basophils in a T cell-independent manner (Moro et al., 2010; Halim et al., 2012; Schmitz et al., 2005; Schneider et al., 2009). Among immune cells, NH cells are needed during an early phase to provide an interface between IL-33 and eosinophilic lung inflammation (Halim et al., 2012; Kondo et al., 2008).

In order to understand the involvement of basophils and mast cells, we employed a genetic approach in which basophils and mast cells can be depleted in BasTRECK mice and MasTRECK mice, respectively, by diphtheria toxin due to the expression of the DT receptor on their cell surface (Sawaguchi et al., 2012). Although basophils are also depleted in MasTRECK mice, basophils quickly recovered within 3 days. Thus, the 7 day delay protocol we used here provided mast cell selective deletion (Figure S4A). Unlike mast cell deletion, following basophil selective deletion, influx of $CD11c^+$ eosinophils into the lung or airways, mucus formation or AHR was no longer observed, although the accumulation of neutrophils was normal (Figures 1B–1E; Figure S4B). Adoptive transfer of wild-type (WT) basophils into the DT-treated BasTRECK mice reconstituted eosinophilic lung inflammation induced by papain treatment (Figures 1B–1D). Taken together, these data demonstrate that basophils have a critical role in papain-induced eosinophilic inflammation.

Our results indicated that IL-33 elicited basophil-mediated lung inflammation. However, macrophage-derived IL-18 and T cell-derived IL-3 have also been reported to be associated with basophil function in the development of allergic responses and protection against parasite infection (Ishikawa et al., 2006) (Shen et al., 2008). However, functional blockade of IL-3 and IL-18, and *Il3* deficiency failed to rescue the papain-induced eosinophilic inflammation (Figures S2D and S2E), confirming that IL-33 is the main initiator in the lung inflammation.

Basophil-Derived IL-4 Promotes Eosinophilic Inflammation

Given that basophils promote eosinophilic inflammation, we sought to test the role of basophil-derived IL-4 in this process. We have previously shown that the basophil-specific *Il4* gene enhancer is located in the region between the 3′UTR and HS4 that previously identified as an IL-4 silencer in T cells (Yagi et al., 2007). To more precisely identify the location of the basophil-specific enhancer, we employed a series of mutant mice lacking each enhancer element in the *Il4-Il13* locus, *Il13* CGRE, *Il4* HS2, *Il4* 3′UTR, and *Il4* HS4-deficient mice (Tanaka et al., 2011). We first analyzed IL-4 production by basophils, mast cells, and NH cells derived from the enhancer-deleted mice. Basophils of *Il4* 3′UTR-deficient mice failed to make IL-4 in response to phorbol myristate acetate (PMA) plus Ionomycin, IL-3, IL-18, and IL-33, but other cytokines were unaffected. Also, there was no effect on IL-4 production by peritoneal or bone-marrow-derived mast cells (BMMCs) (Figures 2A and 2B; Figure S5A). Meanwhile, deletion of HS2 or CNS2 impaired IL-4 production by T cells and mast cells, but not by basophils (Figure 2A) (Tanaka et al., 2011). We also examined IL-13 expression because IL-13 is also known as a critical effector cytokine in lung inflammation and found that the deletion of CGRE abolished IL-13 production by mast cells and NH cells, but not by basophils (Figures 2A and 2C; Figure S5A). The deletion of HS4 has no effect on IL-4 and IL-13 production in either basophils or mast cells (Djuretic et al., 2007) (Tanaka et al., 2011). Consistent with previous results (Moro et al., 2010), NH cells failed to produce IL-4 after stimulation with IL-33 (Figure 2C).

Furthermore, we could show that IL-4 expression was selectively observed in basophils, but not in $CD4^+$ T cells, mast cells, or lung NH cells of papain-treated *Il4* reporter mice (*Il4* h*CD2* Bac Tg) (Figure 2D) (Harada et al., 2012). Eosinophils have been reported to be a source of IL-4 (Oboki et al., 2010), but lung-derived eosinophils secreted no detectable IL-4 protein (Figure 2E; Figure S5B), consistent with a previous report (Sullivan et al., 2011). Taken together, we conclude that IL-4 expression is differentially regulated by distinct enhancers in different cell linages, and that the 3′UTR is a unique enhancer regulating IL-4 expression by basophils, which are the main source of IL-4 in the papain-induced lung inflammation model.

Based on the above results, we considered that mice with a deletion of the *Il4* 3′UTR would be a useful in vivo tool to examine the role of basophil-derived IL-4 in papain-induced lung inflammation. As expected, there was no eosinophil infiltration in the lungs or airways, and reduced mucus formation or AHR in the *Il4* 3′UTR-deficient mice (Figures 3A–3C, 3E, and 3F), but not in *Il4* HS2-deficient mice (Figure S3C). Interestingly, reconstitution with IL-4 secreting WT basophils restored the eosinophilia in *Il4* 3′UTR-deficient mice (Figure 3D), strongly supporting the importance of basophil-derived IL-4 in this response. This phenotype of *Il4* 3′UTR-deficient mice was very similar to that observed in the basophil deletion mice. Furthermore, the deletion of the CGRE element largely impaired mucus formation, but not eosinophil infiltration (Figures 3A–3C), suggesting that IL-13 mainly promotes mucus formation and AHR. These results indicate that basophils play a critical role as a source of IL-4 responsible for papain-induced eosinophilic lung inflammation.

Gene-Expression Profiles of Lung Basophils and Lung NH Cells

Our data indicate that basophils are needed in the interface between papain administration and lung NH cells. To further

(C) Bio-Plex analysis of IL-4, IL-13, IL-5, and IL-6 production by purified NH cells from mesenteries of WT, *Il13* CGRE-deficient, *Il4* HS2-deficient, and *Il4* 3′UTR-deficient mice in response to rIL-33 stimulation for 5 days.

(D) Flow cytometric analysis of the expression of human CD2 (as a reporter of IL-4) in $CD4^+$ T cells ($CD4^+$), basophils ($Fc\varepsilon R1^+CD49b^+c\text{-}Kit^-$), mast cells ($Fc\varepsilon R1^+c\text{-}Kit^+$), and lung NH ($Lin^-Thy1.2^+CD25^+IL7R\alpha^+$) in papain-treated WT and IL4BACTg mice. Results are representative of three independent experiments. Error bars in (A), (B), (C), and (E) represent the SEM.

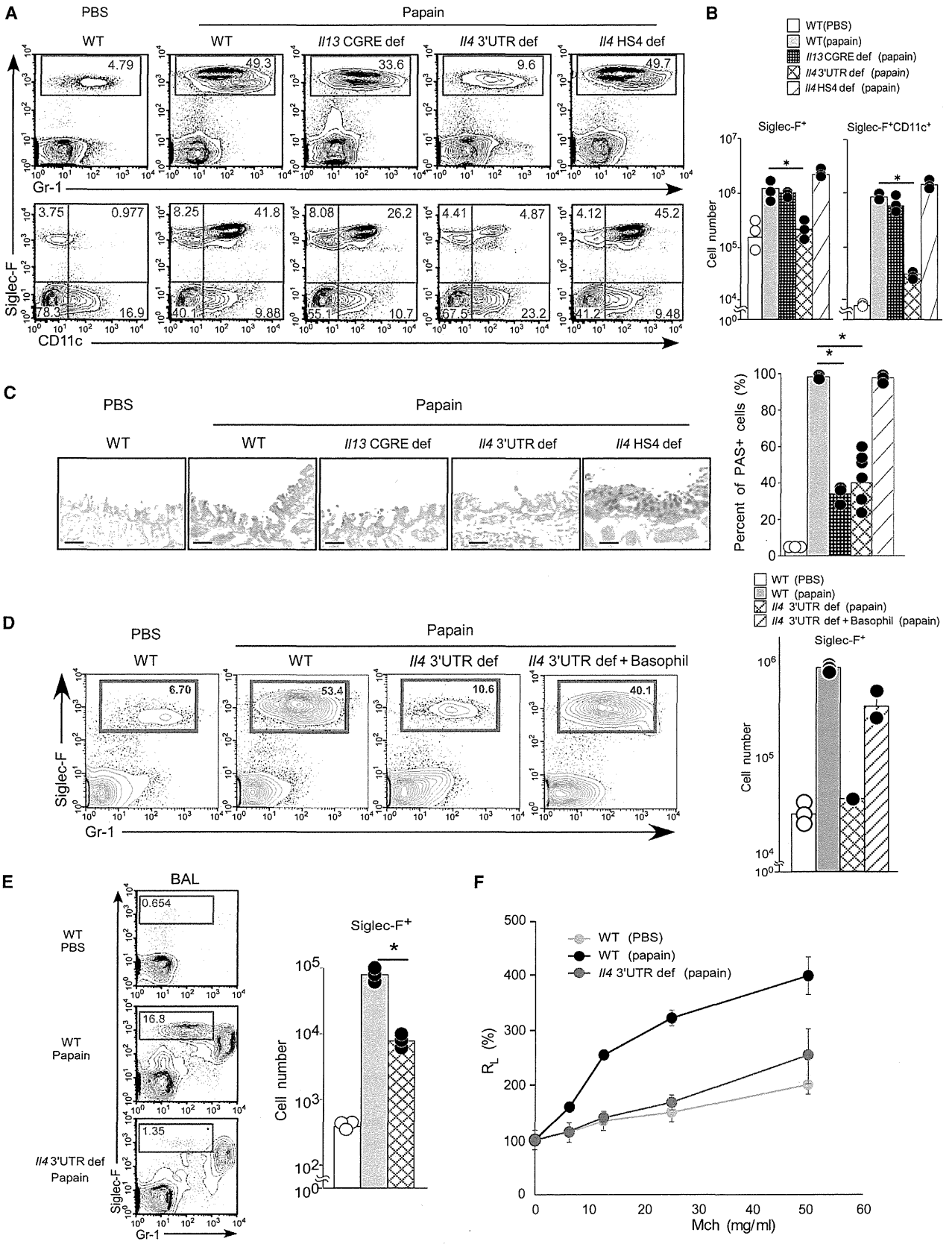

(legend on next page)

characterize the activation status of basophils and NH cells after papain treatment, we characterized global gene-expression patterns of purified lung NH cells before and after treatment by RNA-sequence analysis. We identified basophil populations as CD49b$^+$c-Kit$^-$FcεRI$^+$ cells, and resting basophils consistently expressed high *Il4* transcription (data not shown). Papain treatment resulted in the upregulation of *Il1*, *Il33*, *Tnf*, *Ccl2*, *Ccl3*, *Ccl5*, and *Ccl6* (Figure 4A), and also increased the expression of antibacterial peptides (*S100a8* and *S100a9*), complement components (*C1ra*, *C1s*, and *C2*), and chitinases (*Chi3l4*).

The gene-expression profile of resting lung NH cells was quite similar to the originally described NH cells derived from Fat-associated lymphoid cluster (FALC), which showed high *Gata3*, *Nr4a1*, *Il5*, and *Il13* expression and low transcription of *Notch1* and *Rorc* (Moro et al., 2010) (Figure 4B). Lung NH cells expressed the genes encoding the cytokine receptors for IL-2 (*Il2ra* and *Il2rg*), IL-4 (*Il4ra*), IL-25 (*Il17rb*), IL-7 (*Il7ra*), and IL-33 (*Il1rl1*) as FALC NH cells. In lung NH cells, papain treatment resulted in the upregulation of genes related to cell-cycle progression (*Brac1*, *Cdc*, and *Kif*), cytokines (*Il5* and *Il13*), and chemokines (*Ccl2*, *Ccl8*, *Ccl11*, *Ccl17*, *Ccl22*) (Figure 4C). Taken together, these results indicate that papain treatment can convert NH cells into an effector phenotype via the activation of basophils in the lung.

IL-4 Regulates the Activation of Lung NH Cells

The data from the mice lacking the 3′UTR indicated that basophil-derived IL-4 is responsible for the activation of lung NH cells. Indeed, NH cells constitutively express the IL-4 receptor on their cell surface (Figure 5A), and IL-4Rα mRNA expressions were selectively higher than those of basophils and eosinophils (Figure 5B). Therefore, NH cells seemed a likely target of IL-4 derived from basophils. To directly assess a possible role of IL-4 on NH cell activation during the early phase, we isolated lung NH cells and cultured them with IL-4 for 48 hr. IL-4 treatment upregulated the expression of IL-9, IL-13, CCL11, CCL5, and CCL3 protein in lung NH cells regardless of the presence of IL-33 and IL-2 (Figure 5C). In lung NH cells, IL-4 alone induced low but detectable IL-5 production, and IL-33 synergistically enhanced this effect, indicating that lung NH cells have different mechanisms regulating the production of IL-5 and other type 2 cytokines such as IL-9 and IL-13 during the early phase. Note that IL-33 alone can induce the production of IL-13, as well as IL-5 in the later phase (Kabata et al., 2013). We further assessed the role of IL-13 on lung NH cells, but NH cells failed to respond to IL-13 because of lower expression of the IL-13 receptor (Figure 5B; Figure S6).

Based on dot plot analysis of forward (FSC) versus side scatter (SSC), lung NH cells were activated in papain-treated control and *Il4* HS4-deficient mice producing normal amounts of IL-4. However, NH cells from *Il4* 3′UTR-deficient mice had fewer large cells even after papain treatment (Figure 5D). Consistent with this result, *Il4* 3′UTR-deficient mice, as well as mice depleted basophils, had no increase in NH cell numbers after papain treatment in the lung (Figure 5E; Figure S4B). We further examined whether IL-4 directly led to the proliferation of lung NH cells. Highly purified NH cells from the lung were cultured in the presence of IL-4 combined with IL-2 and IL-33. IL-33 markedly enhanced cell proliferation in combined with IL-2. Interestingly, addition of IL-4 into the IL-2 plus IL-33 cultures further increased the proliferation (Figure 5F). Taken together, IL-4 partially involved in cell proliferation of lung NH cells, but only in the presence of IL-2 and IL-33.

Basophil-Derived IL-4 Promotes Papain-Induced Lung Inflammation

To further confirm a role of basophil-derived IL-4 in the papain-induced inflammation, we reconstituted the DT-treated BasTRECK mice by adaptive transfer of *Il4*$^{-/-}$ basophils. There was no influx of CD11c$^+$Siglec-F$^+$ eosinophils into either the lung or airways of the basophil deleted BasTRECK mice, and this defect was corrected by basophils from WT but not *Il4*$^{-/-}$ mice (Figure 6A). Basophil-deficient mice that were transferred with *Il4*$^{-/-}$ basophils showed a reduction of numbers of lung NH cells compared to control mice upon papain treatment (Figure 6A). The basophil deleted mice and the mice transferred with *Il4*$^{-/-}$ basophils also failed to induce mucus formation (Figure 6B). These results indicate that basophil-derived IL-4 promotes papain-induced lung inflammation through the activation of NH cells in the lung.

DISCUSSION

T cells are generally essential for eosinophilic lung inflammation in an asthmatic reaction, whereas protease allergens induce acute eosinophilic inflammation by a T cell-independent mechanism. Indeed, i.n. administration of papain, a causative agent of occupational asthma, causes eosinophilia, mucus formation, and elevation of IL-5 and IL-13 in BAL of B and T cell-deficient *Rag1*$^{-/-}$ mice (Oboki et al., 2010) and of Il4 HS2-deficient mice as shown here. The involvement of innate cells is further demonstrated by the finding that NH cells, a member of ILC2s, but not Th cells, are the main source of IL-5 and IL-13 in lung explant cultures treated with papain (Halim et al., 2012), and these type 2 cytokines are tightly associated with eosinophilic inflammation. This is consistent with previous studies showing that

Figure 3. Basophil-Derived IL-4 Promotes Eosinophilic Lung Inflammation

(A) Flow cytometric analysis of eosinophils in the lungs of papain-treated WT, *Il13* CGRE-deficient, *Il4* 3′UTR-deficient and *Il4* HS4-deficient mice.

(B) The quantification of lung eosinophils (SiglecF$^+$ and SiglecF$^+$CD11c$^+$).

(C) PAS staining of lung tissues. Scale bars represent 50 μm (left). The percentage of PAS-positive cells in the indicated mice (right). The bars in the graph are labeled as in (B).

(D) Flow cytometric analysis of eosinophils (left) and a quantification of eosinophils in WT and *Il4* 3′UTR-deficient mice unreconsitituted or reconstituted with basophils from the lungs of papain-treated WT mice.

(E) Flow cytometric analysis of eosinophils (left) and the quantification of eosinophils (SiglecF$^+$) in the BAL fluid of the indicated mice. The bars in the graph are labeled as in (B). (right).

(F) AHR to Mch in WT or *Il4* 3′UTR-deficient mice after papain treatment. Dot plots are shown on cells gated out PI$^+$Autfluorescence$^+$Gr1^{hi} (A), (D), or PI$^+$Autfluorescence$^+$ (E). Results are representative of three independent experiments. Error bars in (B)–(E) represent the SEM.

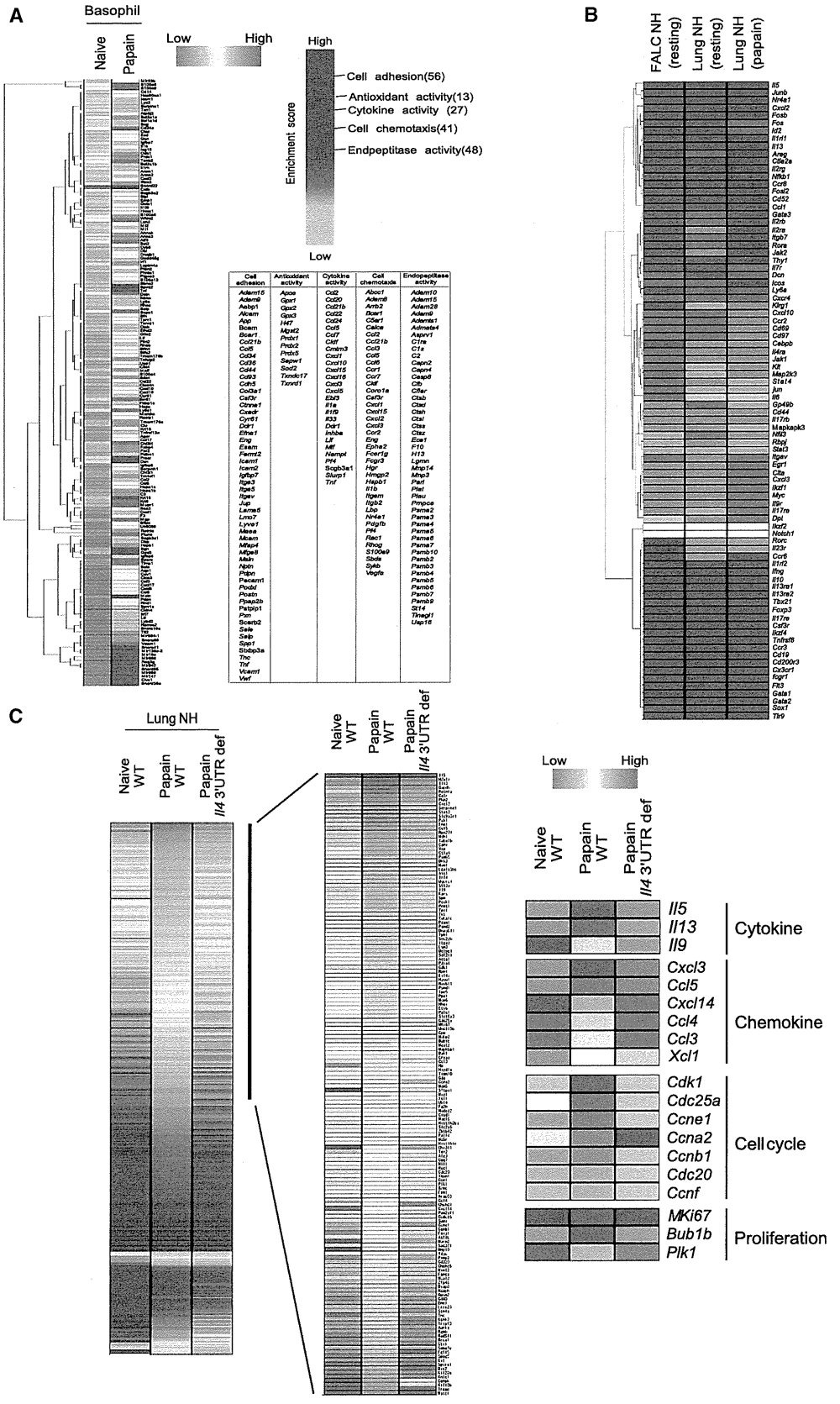

(legend on next page)

Il4$^{-/-}$ *Il13*$^{-/-}$ double-deficient mice do not develop papain-induced inflammation (Oboki et al., 2010). Cysteine proteases are important components of many allergens (Reed and Kita, 2004) and are thought to directly act on airway epithelial cells (Asokananthan et al., 2002) and the activated epithelial cells then release cytokines including TSLP, IL-25, and IL-33 (Strickland et al., 2010). IL-33 is constitutively expressed in endothelial and epithelial cells and is released as an alarmin when cells are damaged (Moussion et al., 2008). *Il33*$^{-/-}$ mice, but not *Tslpr*$^{-/-}$ mice, failed to develop papain-induced eosinophilia or lung inflammation (Oboki et al., 2010). Furthermore, antibody neutralization of IL-33 effectively blocks IL-13 production (Halim et al., 2012). Therefore, it has been speculated that lung NH cells respond to IL-33 produced by activated lung stromal cells, which directly induces IL-5 and IL-13 production by NH cells, resulting in lung eosinophilia, goblet cell hyperplasia, and mucus production (Oboki et al., 2010); (Halim et al., 2012).

Our data clearly demonstrate that basophils and basophil-derived IL-4 are involved in the activation of NH cells capable of secreting high IL-5 and IL-13 in the inflammatory site. The inductive effect of IL-4 on IL-5 production during the early phase was greatly accelerated in the presence of IL-33, indicating that IL-5 and IL-13 are differentially regulated in lung NH cells by IL-4, although longer exposure to IL-33 can induce both IL-5 and IL-13 production by lung NH cells (Kabata et al., 2013). In mice with diphtheria toxin-based genetic depletion of basophils, as well as mice lacking basophil-derived IL-4, the expression of IL-5 and IL-13 was limited as was the development of lung eosinophilia and goblet cell hyperplasia. Therefore, IL-4 secreted from papain-activated basophils plays a pivotal role, inducing a high expression of type 2 cytokines from lung NH cells and expanding their cell numbers during the early phase of the inflammatory response, ultimately resulting in eosinophilic inflammation associated with lung eosinophilia and goblet cell hyperplasia, during the papain induced asthmatic reaction.

The importance of basophils has been reported in chronic allergic dermatitis, and the food-allergy-associated inflammatory disease, eosinophilic esophagitis (Hill et al., 2012; Noti et al., 2013). It has been reported that cysteine proteases induce high IL-4 in mouse basophils (Kamijo et al., 2013). Moreover, Phillips et al. (2003) have reported that in vitro stimulation of human basophils with Derp1 induces IL-4 expression (Phillips et al., 2003). IL-4 and/or IL-13 are known to be an essential cytokine for eosinophilic inflammation in the asthmatic reaction, because airway eosinophilia in double-deficient mice of *Il4* and *Il13* is impaired after short-term administration of papain (Oboki et al., 2010). The present data demonstrate that basophil-derived IL-4 plays a central role by promoting NH function during effector phase. In fact, impairment of the eosinophilic lung inflammation observed in basophil-depleted mice was restored by transfer of basophils derived from WT but not *Il4*$^{-/-}$ mice. Contrary to our results, it has been reported that depletion of basophils with MAR-1 mAb hardly affected chronic papain induced lung eosinophilia by antigen treatment, even though a small numbers of basophils were still present in the spleen after antibody treatment (Kamijo et al., 2013). This is consistent with the observation that antigen-induced lung inflammation hardly mobilizes NH cells unless IL-33 is provided (Kabata et al., 2013). In our experiments, we confirmed the depletion efficiency in BasTRECK mice and found that i.p. treatment with DT (500 ng/mouse) resulted in complete depletion of DX5^{+}FcεRIα^{+}CD200R3^{+} basophils in the spleen, bone marrow, peripheral blood, and lung, and the depletion remained complete for at least three days after the DT injection (Sawaguchi et al., 2012).

Type 2 cytokine-producing innate lymphoid cells (NH, nuocyte and Ih2, members of ILC2s) exhibits many similar phenotypic characteristics, i.e., they are Lin^{-} and produce Th2 cell-derived cytokines (Moro et al., 2010; Neill et al., 2010; Price et al., 2010; Saenz et al., 2010). ILC2s have been found in several different tissues, including the liver, spleen, and lung (Price et al., 2010). In the lung, NH cells have been reported to be responsible for papain-induced inflammation based on the observation that this inflammatory response occurs in *Rag1*$^{-/-}$ mice, but not *Rag2*$^{-/-}$*Il2rg*$^{-/-}$ mice (Halim et al., 2012). We found that the gene-expression profile of lung NH cells was quite similar to that of FALC NH cells. NH cells constitutively showed high expression of IL-4 receptor. The NH cells isolated from the papain treated mouse lung had gene signatures related to effector functions including eosinophilia. Several of these induced genes were IL-4-dependent, because these genes were markedly downregulated in the papain-activated basophils isolated from *Il4* 3′UTR mice. IL-4 specifically influenced not only the expression in NH cells of IL-5, IL-9, IL-13, CCL11, CCL5, and CCL3, which are tightly associated with eosinophilia, but also the cellular expansion of the NH cells. Previous reports have shown that IL-5 and IL-13 expression by NH cells is largely dependent on IL-2+IL-25 and/or IL-33 signaling pathways (Moro et al., 2010), and this also seems to be the case for lung NH cells (Halim et al., 2012). However, IL-4 also controls type 2 cytokine expression and growth of lung NH cells during the early phase of activation.

By using GFP reporter transgenic mice, we have previously shown that transcription of the *Il4* gene in mast cells and basophils is independently regulated by CNS-2 and 3′UTR+HS4 elements, respectively (Yagi et al., 2007). The current deletion mutant analyses indicate that the basophil-specific enhancer is located in the 3′UTR. Therefore, deletion of the 3′UTR caused decreased IL-4 expression only in basophils, but not in Th2 cells

Figure 4. Gene-Expression Profiles of Lung Basophils and Lung NH Cells

(A) Heat-map presentation of gene-expression profiles of the top 100 genes upregulated in basophils from papain-treated mice compared to resting basophils from naive mice (red, high; blue, low) (left). Functional classification of the gene-expression signatures of basophils (twofold or more upregulated genes) according to terms from the Gene Ontology project (GO term), analyzed with the DAVID database of functional annotation tools and presented as significance of enrichment (light blue, $p < 0.05$; blue, $p < 0.0004$) (middle).

(B) Heat-map presentation of gene-expression profiles of FALC NH cells, lung NH cells from naive mice and papain-treated mice.

(C) Heat-map presentation of genes upregulated by papain treatment in lung NH cells from WT and *Il4* 3′UTR-deficient mice (left). The data are indicated the downregulated genes in lung NH from *Il4* 3′UTR-deficient mice compared to WT mice (red, high; blue, low) (middle). Heat-map presentation of expression of genes related to cytokines, chemokines, cell cycle, and proliferation (right). Results in (A) and (B) are representative of two independent experiments.

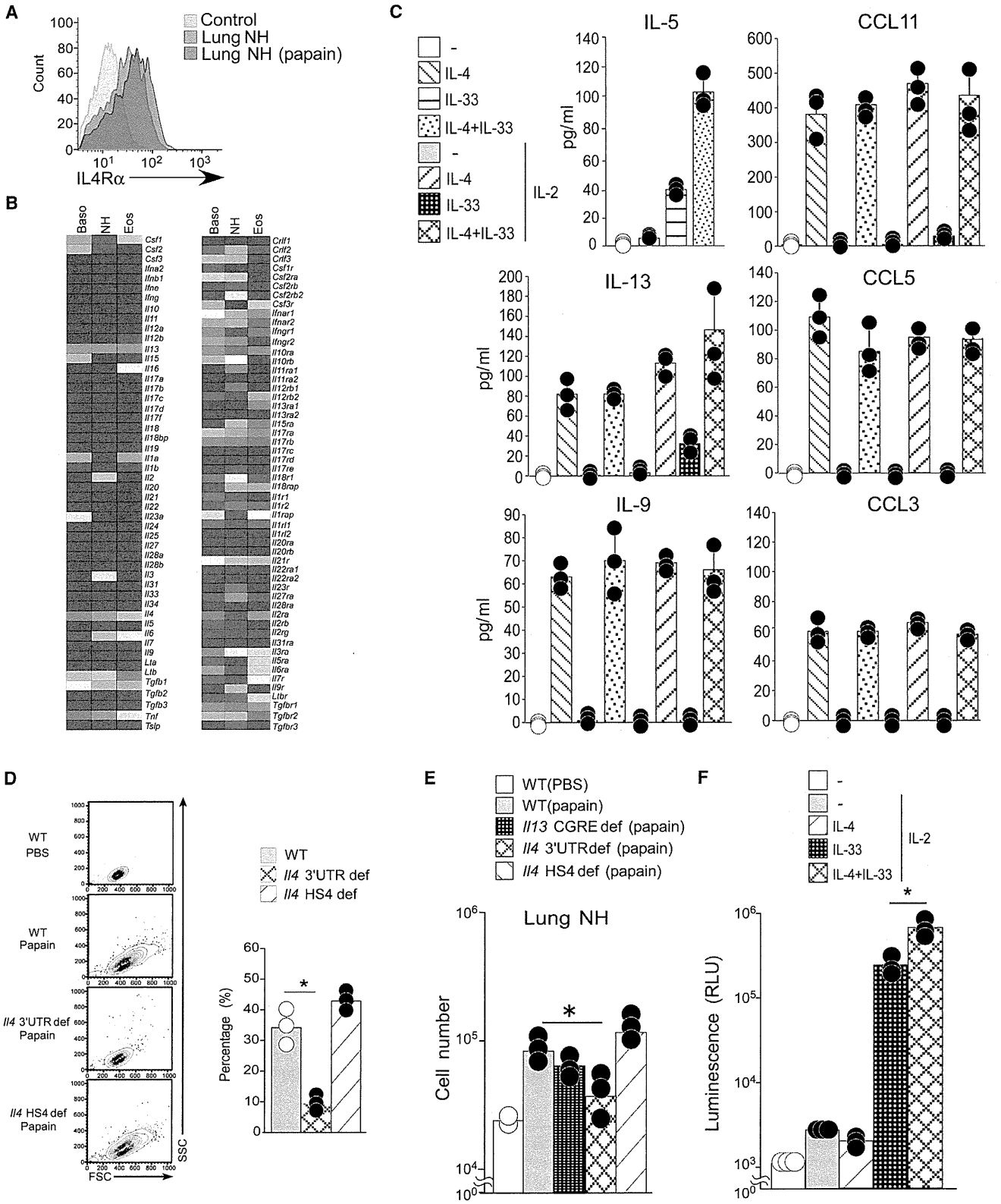

Figure 5. IL-4 Regulates Activation of Lung NH Cells

(A) Flow cytometric analysis of IL-4Rα expression on lung NH cells from naive and papain-treated WT mice.

(B) Heat-map presentation of expression of cytokine and cytokine receptor genes in basophils, NH cells, and eosinophils from the lung of WT mice (red, high; blue, low). Results are representative of two independent experiments.

(legend continued on next page)

or mast cells (Tanaka et al., 2011). Deletion of HS2 and/or CNS2 caused marked reduction of IL-4 in Tfh, Th2, and mast cells, but not basophils (Tanaka et al., 2006; Solymar et al., 2002), and the CGRE deletion caused a marked reduction of IL-13 production by Th2 cells, mast cells, and NH cells (Furusawa et al., 2013), but not basophils. Therefore, the 3′UTR deletion mice are a useful tool to examine the specific function of the IL-4 secreted by basophils in vivo, regardless of the influence of other type 2 cytokines.

In conclusion, basophil plays an important role through IL-4 production in early eosinophilic airway inflammation induced by proteases. IL-4 binding to its cognate receptor on NH is critical to initiate IL-5, IL-9, and IL-13 expression and release of chemoattractants that are required for eosinophilia in the lung. Therefore, the network composed of innate immune cells, including basophils and NH cells, is important for the lung immune system to elicit a rapid response to infection.

EXPERIMENTAL PROCEDURES

Mice

BasTRECK and MasTRECK mice have been described previously (Sawaguchi et al., 2012). For DT treatment, mice were injected intraperitoneally with 250 ng of DT in 250 μl of PBS per mouse for MasTRECK mice or 500 ng of DT in 250 μl of PBS per mouse for BasTRECK mice. CGRE, HS2, 3′UTR, HS4, and CNS2-deficient mice, *Il4*BACTg, and *Il33*$^{-/-}$ mice have also been described in previous reports (Harada et al., 2012; Oboki et al., 2010; Tanaka et al., 2011). *Il13*^{Tomato} mice, *Il4*$^{-/-}$ mice, and *Tslpr*$^{-/-}$ mice on a C57BL/6J background were kindly provided by Dr. McKenzie (Barlow et al., 2012), Dr. M. Kopf (Kopf et al., 1993), and Dr. Zieglar (Carpino et al., 2004), respectively. *Il3*-deficient mice on a BALB/c background (RBRC02298) were provided by RIKEN BRC through the National BioResource Project of the MEXT, Japan (Mach et al., 1998). Mice were housed under specific pathogen-free conditions and in accordance with the guidelines of the Institutional Animal Care Committee of the RIKEN.

Airway Inflammation and Airway Hypersensitivity

Mice were treated i.n. with 20 μl of 30 μg HDM extract (LSL) in saline or saline alone on 7 consecutive days. For papain, mice were treated i.n. with 20 μl of 50 μg papain (Sigma Aldrich) in saline or saline alone on 3 consecutive days. At 24 hr after the last instillation, bronchoalveolar lavage (BAL) fluids and lungs were collected for examination of the BAL or lung cell profiles and lung histology. For AHR, acetylcholine-dependent AHR in treated mice was measured as described previously (Seki et al., 2003).

Antibodies

Phycoerythrobilin (PE)-conjugated anti- Siglec-F, FITC-conjugated anti-Thy1.2, CD49b, CD11b, CD69, Allophycocyanin (APC)-conjugated anti-CD117, CD44, α-GalCer loaded CD1d dimer, biotinylated anti-NK1.1,CD62L antibodies were purchased from BD Biosciences, and PE-conjugated anti-FcεR1, IL7Rα,IL4Rα, FITC-conjugated anti-F4/80, APC-conjugated anti-CD11c, biotinylated anti-CD3ε, CD19, CD11b, CD11c, Gr-1, Ter119, PerCP-cy5.5 conjugated streptavidin were purchased from eBioscience. PerCP-cy5.5 conjugated anti-CD25 and biotinylated anti-human CD2, CXCR3 antibodies were purchased from BioLegend. APC conjugated anti-CCR2 antibody was purchased from R&D systems. Purified anti-IL-18, anti-IL-3, and isotype IgG1κ for neutralization assay were purchased from MBL and BioLegend, respectively. Propidium iodide (PI) was used to exclude nonviable cells. A BD FACS Aria II (BD Biosciences) was used for cell sorting and phenotypic analysis and Flowjo v. 8.6 (Tree Star) was used for data analysis.

Cell Preparation and Reconstitution of Basophils

Lungs from mice were minced with scissors in RPMI-1640^{+} containing 10% FBS. Minced lungs were incubated RPMI-1640 containing 10% FBS, 400U collagenase IV and 50 mg/ml DNase I for 1 hr at 37°C. Digested tissues were passed through a strainer. Cells were used for analysis by flow cytometry after lysis of red blood cells. For cell sorting, basophil (FcεRI^{+}CD49b^{+}c-Kit^{-}), NH cell (Lin^{-}Thy1.2^{+}CD25^{+}IL7Rα^{+}), and eosinophil (CD11c^{+} or CD11c^{-}SiglecF^{+}Gr-1^{lo} autofluorescence^{-}) were sorted from lung cells by BD FACS Aria II (BD Biosciences). For BMMC, bone marrow cells were cultured in the presence of rIL-3 for 4 weeks. For reconstitution of basophils, lung basophils were isolated from mice that i.n. administrated with papain for three days. Lung basophils (1×10^4 cells) were intravenously administrated into mice before papain treatment.

Measurement of Cytokine Production

Cytokines were measured by a suspension array system (Luminex 200; Bio-Rad Laboratories).

RNA Sequence

Total RNA was isolated with TRIzol and 1 μg of isolated RNA were used for production of the RNA-Seq cDNA library with NEBNext Ultra RNA Library Prep Kit for Illumina (NEB Biolabs) according to the manufacturer's protocol that included cDNA synthesis and fragmentation, the addition of adaptors, size selection, amplification, and quality control. A HiSeq 1500 system (Illumina) was used for SE-50 sequencing (single-ended 50 base-pair reads). Basic data analysis was done with CLC Biosystems Genomic Workbench) analysis programs (CLC Biosystems) to generate quantitative data for all genes, including reads per kilobase of exon per million mapped reads, unique and total gene reads, annotated transcripts and detected transcripts, median coverage, chromosomal location, and putative exons. Heat maps were produced by normalization of the reads per kilobase of exon per million mapped reads for each gene across all treatment conditions, followed by the generation of hierarchy clustered heat maps with MeV (http://www.tm4.org/mev.html).

Histological Analysis

Lungs were fixed in 4% (vol/vol) paraformaldehyde, infused with 20% sucrose and embedded in OTC compound (Sakura Finetek) for frozen sections. Frozen sections of lung were cut (5 μm) for PAS staining. For quantification of staining with PAS, mucus production was assessed by the frequency of epithelial cells that stained strongly positive. Individual slides were examined independently.

Statistical Analysis

A two-tailed Student's t test was used for statistical analysis. Differences with a p value of less than 0.05 were considered significant. * $p < 0.05$

ACCESSION NUMBER

RNA-seq data in this work are available in the Gene Expression Omnibus (GEO) database (http://www.ncbi.nlm.nih.gov/gds) under the accession number GSE56292.

SUPPLEMENTAL INFORMATION

Supplemental Information includes six figures and Supplemental Experimental Procedures and can be found with this article online at http://dx.doi.org/10.1016/j.immuni.2014.04.013.

(C) Bio-Plex analysis of cytokine and chemokine production by lung NH cells (1,000 cells/sample) in response to the indicated stimuli for 48 hr.
(D) Flow cytometry analysis of forward scatter (FSC) and side scatter (SSC) of lung NH cells from the indicated mice after treatment with PBS or papain (left). The percentage of lung NH cells with high FSC/SSC in the indicated papain-treated mice after subtracting that in naive mice (right).
(E) Quantification of NH cells in lungs of WT, *Il13* CGRE-deficient, *Il4* 3′UTR-deficient, and *Il4* HS4-deficient mice administrated papain i.n. continuously for 3 days.
(F) Viability of lung NH cells cultured for 7 days in the presence of the indicated cytokines. Results in (A), (C), (D), (E), and (F) are representative of three independent experiments. Error bars in (C)–(F) represent the SEM.

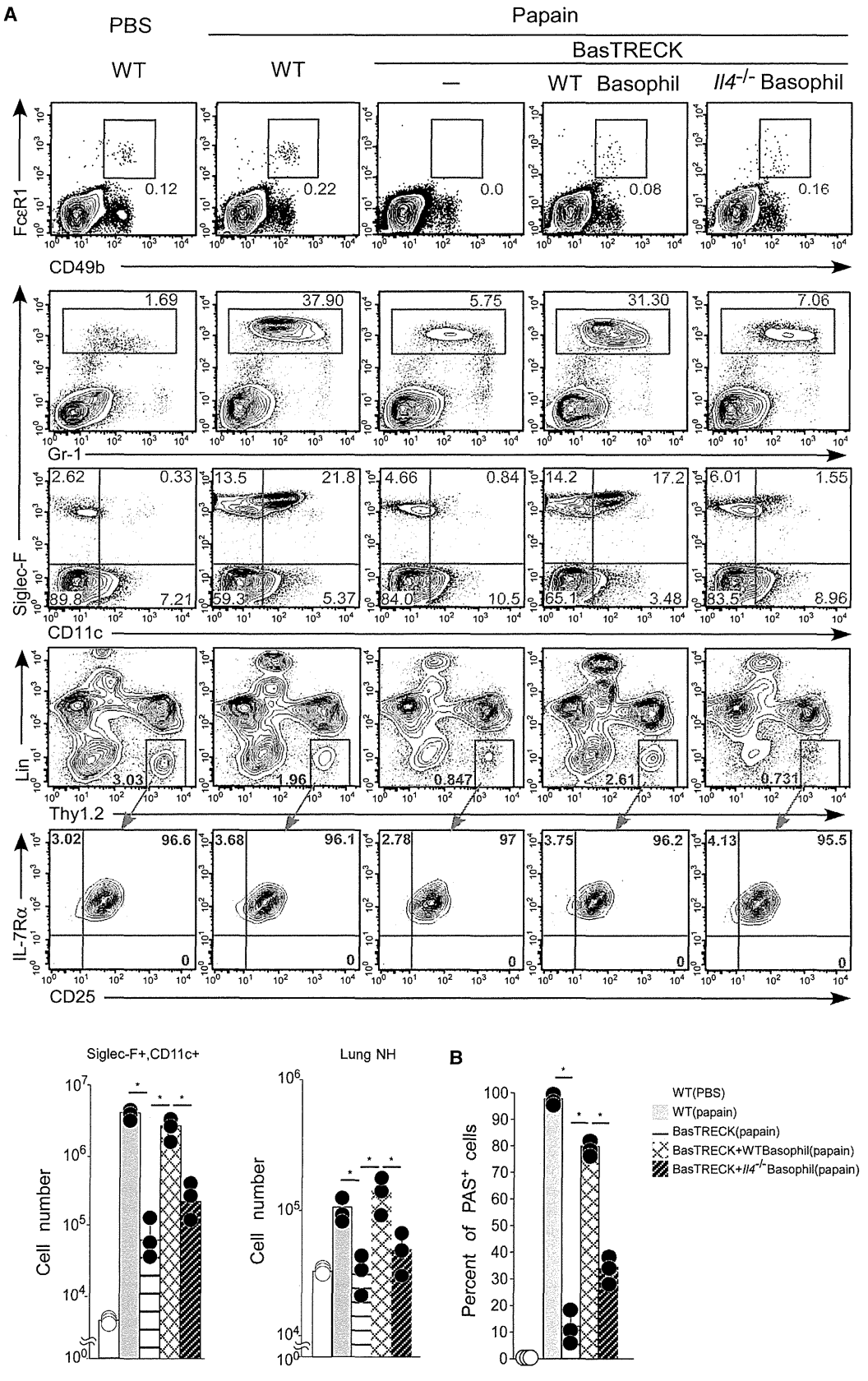

(legend on next page)

ACKNOWLEDGMENTS

We thank H. Fujimoto, Y. Hachiman, Y. Suzuki, S. Law, C. Ohashi, N. Takeno, and M. Mochizuki for technical support and animal maintenance. We thank P. Burrows for helpful comments on the manuscript. This work was supported by a Grant-in-Aid for Scientific Research on Innovative Areas (23118526) to K.M. from the Ministry of Education, Culture, Sports, Science, and Technology (MEXT) of Japan, a Grant-in-Aid for Scientific Research (A) (24249058) to M.K., a Grant-in Aid for Young Scientist (A) (22689013) to K.M., a Grant-in-Aid for Scientific Research (S) (22229004) to S.K. from the Japan Society for the Promotion of Science (JSPS), the Program for Promotion of Fundamental Studies in Health Sciences of the National Institute of Biomedical Innovation (NIBIO) to K.M., Precursory Research for Embryonic Science and Technology (PRESTO) to K.M. from the Japan Science and Technology Agency (JST), and a grant from the Takeda Foundation to M.K.

Received: October 22, 2013
Accepted: April 22, 2014
Published: May 15, 2014

REFERENCES

Asokananthan, N., Graham, P.T., Stewart, D.J., Bakker, A.J., Eidne, K.A., Thompson, P.J., and Stewart, G.A. (2002). House dust mite allergens induce proinflammatory cytokines from respiratory epithelial cells: the cysteine protease allergen, Der p 1, activates protease-activated receptor (PAR)-2 and inactivates PAR-1. J. Immunol. *169*, 4572–4578.

Barlow, J.L., Bellosi, A., Hardman, C.S., Drynan, L.F., Wong, S.H., Cruickshank, J.P., and McKenzie, A.N. (2012). Innate IL-13-producing nuocytes arise during allergic lung inflammation and contribute to airways hyperreactivity. J Allergy Clin Immunol *129*, 191-198 e191-194.

Carpino, N., Thierfelder, W.E., Chang, M.S., Saris, C., Turner, S.J., Ziegler, S.F., and Ihle, J.N. (2004). Absence of an essential role for thymic stromal lymphopoietin receptor in murine B-cell development. Mol. Cell. Biol. *24*, 2584–2592.

Chang, Y.J., Kim, H.Y., Albacker, L.A., Baumgarth, N., McKenzie, A.N., Smith, D.E., Dekruyff, R.H., and Umetsu, D.T. (2011). Innate lymphoid cells mediate influenza-induced airway hyper-reactivity independently of adaptive immunity. Nat. Immunol. *12*, 631–638.

Coffman, R.L., Ohara, J., Bond, M.W., Carty, J., Zlotnik, A., and Paul, W.E. (1986). B cell stimulatory factor-1 enhances the IgE response of lipopolysaccharide-activated B cells. J. Immunol. *136*, 4538–4541.

Djuretic, I.M., Levanon, D., Negreanu, V., Groner, Y., Rao, A., and Ansel, K.M. (2007). Transcription factors T-bet and Runx3 cooperate to activate Ifng and silence Il4 in T helper type 1 cells. Nat. Immunol. *8*, 145–153.

Furusawa, J., Moro, K., Motomura, Y., Okamoto, K., Zhu, J., Takayanagi, H., Kubo, M., and Koyasu, S. (2013). Critical role of p38 and GATA3 in natural helper cell function. J. Immunol. *191*, 1818–1826.

Gregory, L.G., and Lloyd, C.M. (2011). Orchestrating house dust mite-associated allergy in the lung. Trends Immunol. *32*, 402–411.

Halim, T.Y., Krauss, R.H., Sun, A.C., and Takei, F. (2012). Lung natural helper cells are a critical source of Th2 cell-type cytokines in protease allergen-induced airway inflammation. Immunity *36*, 451–463.

Hamelmann, E., and Gelfand, E.W. (2001). IL-5-induced airway eosinophilia—the key to asthma? Immunol. Rev. *179*, 182–191.

Harada, Y., Tanaka, S., Motomura, Y., Harada, Y., Ohno, S., Ohno, S., Yanagi, Y., Inoue, H., and Kubo, M. (2012). The 3′ enhancer CNS2 is a critical regulator of interleukin-4-mediated humoral immunity in follicular helper T cells. Immunity *36*, 188–200.

Hill, D.A., Siracusa, M.C., Abt, M.C., Kim, B.S., Kobuley, D., Kubo, M., Kambayashi, T., Larosa, D.F., Renner, E.D., Orange, J.S., et al. (2012). Commensal bacteria-derived signals regulate basophil hematopoiesis and allergic inflammation. Nat. Med. *18*, 538–546.

Ishikawa, Y., Yoshimoto, T., and Nakanishi, K. (2006). Contribution of IL-18-induced innate T cell activation to airway inflammation with mucus hypersecretion and airway hyperresponsiveness. Int. Immunol. *18*, 847–855.

Kabata, H., Moro, K., Fukunaga, K., Suzuki, Y., Miyata, J., Masaki, K., Betsuyaku, T., Koyasu, S., and Asano, K. (2013). Thymic stromal lymphopoietin induces corticosteroid resistance in natural helper cells during airway inflammation. Nature communications *4*, 2675.

Kaiko, G.E., and Foster, P.S. (2011). New insights into the generation of Th2 immunity and potential therapeutic targets for the treatment of asthma. Curr. Opin. Allergy Clin. Immunol. *11*, 39–45.

Kamijo, S., Takeda, H., Tokura, T., Suzuki, M., Inui, K., Hara, M., Matsuda, H., Matsuda, A., Oboki, K., Ohno, T., et al. (2013). IL-33-mediated innate response and adaptive immune cells contribute to maximum responses of protease allergen-induced allergic airway inflammation. J. Immunol. *190*, 4489–4499.

Kim, H.Y., DeKruyff, R.H., and Umetsu, D.T. (2010). The many paths to asthma: phenotype shaped by innate and adaptive immunity. Nat. Immunol. *11*, 577–584.

Kondo, Y., Yoshimoto, T., Yasuda, K., Futatsugi-Yumikura, S., Morimoto, M., Hayashi, N., Hoshino, T., Fujimoto, J., and Nakanishi, K. (2008). Administration of IL-33 induces airway hyperresponsiveness and goblet cell hyperplasia in the lungs in the absence of adaptive immune system. Int. Immunol. *20*, 791–800.

Kopf, M., Le Gros, G., Bachmann, M., Lamers, M.C., Bluethmann, H., and Köhler, G. (1993). Disruption of the murine IL-4 gene blocks Th2 cytokine responses. Nature *362*, 245–248.

Kroeger, K.M., Sullivan, B.M., and Locksley, R.M. (2009). IL-18 and IL-33 elicit Th2 cytokines from basophils via a MyD88- and p38alpha-dependent pathway. J. Leukoc. Biol. *86*, 769–778.

Lloyd, C.M., and Hessel, E.M. (2010). Functions of T cells in asthma: more than just T(H)2 cells. Nat. Rev. Immunol. *10*, 838–848.

Mach, N., Lantz, C.S., Galli, S.J., Reznikoff, G., Mihm, M., Small, C., Granstein, R., Beissert, S., Sadelain, M., Mulligan, R.C., and Dranoff, G. (1998). Involvement of interleukin-3 in delayed-type hypersensitivity. Blood *91*, 778–783.

Moro, K., Yamada, T., Tanabe, M., Takeuchi, T., Ikawa, T., Kawamoto, H., Furusawa, J., Ohtani, M., Fujii, H., and Koyasu, S. (2010). Innate production of T(H)2 cytokines by adipose tissue-associated c-Kit(+)Sca-1(+) lymphoid cells. Nature *463*, 540–544.

Moussion, C., Ortega, N., and Girard, J.P. (2008). The IL-1-like cytokine IL-33 is constitutively expressed in the nucleus of endothelial cells and epithelial cells in vivo: a novel 'alarmin'? PLoS ONE *3*, e3331.

Neill, D.R., Wong, S.H., Bellosi, A., Flynn, R.J., Daly, M., Langford, T.K., Bucks, C., Kane, C.M., Fallon, P.G., Pannell, R., et al. (2010). Nuocytes represent a new innate effector leukocyte that mediates type-2 immunity. Nature *464*, 1367–1370.

Noti, M., Wojno, E.D., Kim, B.S., Siracusa, M.C., Giacomin, P.R., Nair, M.G., Benitez, A.J., Ruymann, K.R., Muir, A.B., Hill, D.A., et al. (2013). Thymic stromal lymphopoietin-elicited basophil responses promote eosinophilic esophagitis. Nat. Med. *19*, 1005–1013.

Figure 6. Basophil-Derived IL-4 Controls Papain-Induced Lung Inflammation

(A) Flow cytometric analysis of basophils, eosinophils, and NH cells in the lungs of papain-treated WT and BasTRECK mice unreconsitituted or reconstituted with WT or IL-$4^{-/-}$ basophils following DT treatment. Dot plots of FcεR1, CD49b, and siglec-F are shown on cells gated out PI^{+}c-Kit+ and PI^{+}Autfluorescence^{+}$Gr1^{hi}$, respectively (upper). The quantification of $CD11c^{+}$ eosinophils and NH cells in the lungs of indicated mice (lower).

(B) The percentage of PAS-positive cells in PAS staining of lung tissue from the same mice as in (A). Results are representative of three independent experiments. Error bars represent the SEM.

Novey, H.S., Marchioli, L.E., Sokol, W.N., and Wells, I.D. (1979). Papain-induced asthma—physiological and immunological features. J. Allergy Clin. Immunol. *63*, 98–103.

Oboki, K., Ohno, T., Kajiwara, N., Arae, K., Morita, H., Ishii, A., Nambu, A., Abe, T., Kiyonari, H., Matsumoto, K., et al. (2010). IL-33 is a crucial amplifier of innate rather than acquired immunity. Proc. Natl. Acad. Sci. USA *107*, 18581–18586.

Ohnmacht, C., Schwartz, C., Panzer, M., Schiedewitz, I., Naumann, R., and Voehringer, D. (2010). Basophils orchestrate chronic allergic dermatitis and protective immunity against helminths. Immunity *33*, 364–374.

Phillips, C., Coward, W.R., Pritchard, D.I., and Hewitt, C.R. (2003). Basophils express a type 2 cytokine profile on exposure to proteases from helminths and house dust mites. J. Leukoc. Biol. *73*, 165–171.

Price, A.E., Liang, H.E., Sullivan, B.M., Reinhardt, R.L., Eisley, C.J., Erle, D.J., and Locksley, R.M. (2010). Systemically dispersed innate IL-13-expressing cells in type 2 immunity. Proc. Natl. Acad. Sci. USA *107*, 11489–11494.

Pulendran, B., and Artis, D. (2012). New paradigms in type 2 immunity. Science *337*, 431–435.

Reed, C.E., and Kita, H. (2004). The role of protease activation of inflammation in allergic respiratory diseases. J. Allergy Clin. Immunol. *114*, 997–1008, quiz 1009.

Saenz, S.A., Siracusa, M.C., Perrigoue, J.G., Spencer, S.P., Urban, J.F., Jr., Tocker, J.E., Budelsky, A.L., Kleinschek, M.A., Kastelein, R.A., Kambayashi, T., et al. (2010). IL25 elicits a multipotent progenitor cell population that promotes T(H)2 cytokine responses. Nature *464*, 1362–1366.

Sawaguchi, M., Tanaka, S., Nakatani, Y., Harada, Y., Mukai, K., Matsunaga, Y., Ishiwata, K., Oboki, K., Kambayashi, T., Watanabe, N., et al. (2012). Role of mast cells and basophils in IgE responses and in allergic airway hyperresponsiveness. J. Immunol. *188*, 1809–1818.

Schmitz, J., Owyang, A., Oldham, E., Song, Y., Murphy, E., McClanahan, T.K., Zurawski, G., Moshrefi, M., Qin, J., Li, X., et al. (2005). IL-33, an interleukin-1-like cytokine that signals via the IL-1 receptor-related protein ST2 and induces T helper type 2-associated cytokines. Immunity *23*, 479–490.

Schneider, E., Petit-Bertron, A.F., Bricard, R., Levasseur, M., Ramadan, A., Girard, J.P., Herbelin, A., and Dy, M. (2009). IL-33 activates unprimed murine basophils directly in vitro and induces their in vivo expansion indirectly by promoting hematopoietic growth factor production. J. Immunol. *183*, 3591–3597.

Seki, Y., Inoue, H., Nagata, N., Hayashi, K., Fukuyama, S., Matsumoto, K., Komine, O., Hamano, S., Himeno, K., Inagaki-Ohara, K., et al. (2003). SOCS-3 regulates onset and maintenance of T(H)2-mediated allergic responses. Nat. Med. *9*, 1047–1054.

Shen, T., Kim, S., Do, J.S., Wang, L., Lantz, C., Urban, J.F., Le Gros, G., and Min, B. (2008). T cell-derived IL-3 plays key role in parasite infection-induced basophil production but is dispensable for in vivo basophil survival. Int. Immunol. *20*, 1201–1209.

Sokol, C.L., Barton, G.M., Farr, A.G., and Medzhitov, R. (2008). A mechanism for the initiation of allergen-induced T helper type 2 responses. Nat. Immunol. *9*, 310–318.

Solymar, D.C., Agarwal, S., Bassing, C.H., Alt, F.W., and Rao, A. (2002). A 3′ enhancer in the IL-4 gene regulates cytokine production by Th2 cells and mast cells. Immunity *17*, 41–50.

Spits, H., Artis, D., Colonna, M., Diefenbach, A., Di Santo, J.P., Eberl, G., Koyasu, S., Locksley, R.M., McKenzie, A.N., Mebius, R.E., et al. (2013). Innate lymphoid cells—a proposal for uniform nomenclature. Nat. Rev. Immunol. *13*, 145–149.

Strickland, D.H., Upham, J.W., and Holt, P.G. (2010). Epithelial-dendritic cell interactions in allergic disorders. Curr. Opin. Immunol. *22*, 789–794.

Sullivan, B.M., Liang, H.E., Bando, J.K., Wu, D., Cheng, L.E., McKerrow, J.K., Allen, C.D., and Locksley, R.M. (2011). Genetic analysis of basophil function in vivo. Nat. Immunol. *12*, 527–535.

Tanaka, S., Tsukada, J., Suzuki, W., Hayashi, K., Tanigaki, K., Tsuji, M., Inoue, H., Honjo, T., and Kubo, M. (2006). The interleukin-4 enhancer CNS-2 is regulated by Notch signals and controls initial expression in NKT cells and memory-type CD4 T cells. Immunity *24*, 689–701.

Tanaka, S., Motomura, Y., Suzuki, Y., Yagi, R., Inoue, H., Miyatake, S., and Kubo, M. (2011). The enhancer HS2 critically regulates GATA-3-mediated Il4 transcription in T(H)2 cells. Nat. Immunol. *12*, 77–85.

Tang, H., Cao, W., Kasturi, S.P., Ravindran, R., Nakaya, H.I., Kundu, K., Murthy, N., Kepler, T.B., Malissen, B., and Pulendran, B. (2010). The T helper type 2 response to cysteine proteases requires dendritic cell-basophil cooperation via ROS-mediated signaling. Nat. Immunol. *11*, 608–617.

Tovey, E.R., Chapman, M.D., and Platts-Mills, T.A. (1981). Mite faeces are a major source of house dust allergens. Nature *289*, 592–593.

Wills-Karp, M. (2004). Interleukin-13 in asthma pathogenesis. Immunol. Rev. *202*, 175–190.

Yagi, R., Tanaka, S., Motomura, Y., and Kubo, M. (2007). Regulation of the Il4 gene is independently controlled by proximal and distal 3′ enhancers in mast cells and basophils. Mol. Cell. Biol. *27*, 8087–8097.